This will prevent intramolecular electron transfer. There will be the additional bonus that the substituent effects will, at the same time, decrease the energy of the lowest lying MLCT states and, therefore, the energy gap between the MLCT and ^{3}An states. As the energy gap is lowered, it will be possible to decrease the extent of excited-state energy lost in the intramolecular energy-transfer event.

Acknowledgments are made to the National Science Foundation under Grant CHE-8806664 for support of this research and to the SERC for postdoctoral support for S.B.

Registry No. $[Ru(bpyCH_2OCH_2An)_3][PF_6]_2$, 122020-09-1; $bpyCH_2OCH_2An$, 122020-07-9; $Ru(dmso)_4Cl_2$, 59091-96-2; 9-anthracenemethanol, 1468-95-7; 4-(bromomethyl)-4'-methylbipyridine, 81998-05-2.

(46) Balzani, V.; Tunis, A.; Barigelletti, F.; Belser, P.; Von Zelewsky, A. *Sci. Pap. Inst. Phys. Chem. Res.* **1984**, *78*, 78.
(47) Barqawi, K. R.; Llobet, A.; Meyer, T. J. *J. Am. Chem. Soc.* **1988**, *110*, 7751.

Directional Electron Transfer: Conformational Interconversions and Their Effects on Observed Electron-Transfer Rate Constants

Bruce S. Brunschwig* and Norman Sutin*

Contribution from the Chemistry Department, Brookhaven National Laboratory, Upton, New York 11973. *Received February 17, 1989*

Abstract: The interaction between conformation changes and electron-transfer rates is considered for systems containing two redox centers. The effect of conformation changes on the free-energy barrier to intramolecular electron transfer is examined. Unstable conformers R* of the reactant (or P* of the product) that are either more (low-λ intermediates) or less (high-λ intermediates) redox-active than the stable reactant R (or product P) are considered. The relative energies of the conformers determine whether the observed electron-transfer reaction proceeds by a two-step mechanism involving the intermediate formation of an unstable conformer or by a direct (concerted) reaction involving only the stable reactant and product. In the normal free energy region, reactions with high-λ intermediates never compete with the direct reaction. The low-λ R* mechanism is favorable only at low driving force when the R* intermediates are just slightly less stable than R, while the P* mechanism can be favorable over the entire free energy region. In the inverted free energy region, reactions involving low-λ P* and high-λ R* or P* intermediates can be more rapid than the direct reaction. Such two-step mechanisms can mask the reduction in rate with increasing driving force expected for the direct reaction in the inverted region. The present analysis generates a set of equations that indicate when the two-step or the direct mechanism is energetically favored. Only when the two-step mechanisms are favored is "gating" or conformational control possible. Reactions with rates that explicitly depend upon the "direction" of electron transfer can still be observed even when gating is absent: because the P* mechanism is favorable over a broader range of free energies and stabilities than the R* mechanism, the overall reaction can have different mechanisms for the forward and reverse directions. Thus conformation changes alone can give rise to directional and/or gated electron transfer.

Intramolecular electron transfer within "supramolecular" systems consisting of several redox components[1-4] or within large molecules, such as native and derivatized metalloproteins,[5-9] are of considerable current interest. Such systems allow the study of the effects of distance and driving force on electron-transfer rates and afford a valuable opportunity for testing theoretical models. While these studies are yielding important information, interpretation of the measured rates requires detailed knowledge of the structures of the reactants and products. In addition, possible conformation changes need to be considered:[7,10] directional and/or "gated" electron transfer may be observed in systems where the stable form of the reactant is redox-inactive but where a less stable, but more redox-active, conformer of the reactant is attainable. Alternatively, for reactions in the inverted region, a mechanism involving a relatively redox-inactive conformer may be favorable!

The question of directional electron transfer has been considered by a number of authors. It has recently been invoked to rationalize an "anomalous" rate of the intramolecular electron transfer between the iron and ruthenium centers in a modified cytochrome *c*.[7] The oxidation of the Fe(II) heme by $Ru^{III}(NH_3)_4$(isn) attached to the histidine-33 residue of cytochrome *c* is much slower[7] than the reduction of the Fe(III) heme by a bound $Ru^{II}(NH_3)_5$ moiety[5] despite the very similar driving forces for the two reactions. Isied and co-workers[7] have interpreted this apparent dependence of the rate on direction by proposing that the iron(II) protein undergoes a conformation change prior to its oxidation to iron(III). Hoffman and Ratner[10] have considered the consequences of coupled conformation and electron-transfer reactions and concluded that, for systems with conformational equilibria, the reaction will *always* proceed by a two-step rather than by a concerted mechanism.[10] In this paper we consider multistep electron-transfer reactions and derive the conditions under which a two-step mechanism will be

(1) Hush, N. S.; Paddon-Row, M. N.; Cotsaris, E.; Oevering, H.; Verhoeven, Z. W.; Heppner, M. *Chem. Phys. Lett.* **1985**, *117*, 8-11.
(2) Isied, S. S.; Vassilian, A.; Magnuson, R. H.; Schwarz, H. A. *J. Am. Chem. Soc.* **1985**, *107*, 7432-7438.
(3) Isied, S. S.; Vassilian, A.; Wishart, J. F.; Creutz, C.; Schwarz, H. A.; Sutin, N. *J. Am. Chem. Soc.* **1988**, *110*, 635-637.
(4) Wasilewski, M. R.; Niemczyk, M. P. *ACS Symp. Ser.* **1986**, *321*, 154-165.
(5) Isied, S. S.; Kuehn, C.; Worosila, G. *J. Am. Chem. Soc.* **1984**, *106*, 1722-1726.
(6) Nocera, B. G.; Winkler, J. R.; Yocom, K. M.; Bordignon, D.; Gray, H. B. *J. Am. Chem. Soc.* **1984**, *106*, 5145-5150.
(7) Bechtold, R.; Kuehn, C.; Lepre, C.; Isied, S. *Nature (London)* **1986**, *322*, 286-288.
(8) Liang, N.; Kang, C. H.; Ho, P. S.; Margoliash, D.; Hoffman, B. M. *J. Am. Chem. Soc.* **1986**, *108*, 4665-4666.
(9) Liang, N.; Pielak, G. J.; Mauk, A. G.; Smith, M.; Hoffman, B. M. *Proc. Natl. Acad. Sci. U.S.A.* **1987**, *84*, 1249-1252.
(10) Hoffman, B. M.; Ratner, M. R. *J. Am. Chem. Soc.* **1987**, *109*, 6237-6243.

0002-7863/89/1511-7454$01.50/0

more favorable than the direct reaction. Our conclusions differ from those of Hoffman and Ratner in certain respects.

Although the emphasis in this paper is on protein conformation changes, the formalism is much more general and can also be applied to electron transfers coupled to other types of configurational (structural or electronic) changes. These include, for example, coordination number changes (e.g., octahedral/tetrahedral), linkage isomerizations (e.g., changes from a C- to an N-bonded imidazole), and spin-state changes.

In the case of bimolecular electron-transfer reactions the concentration dependence of the rate can provide information regarding rate-determining structural or electronic changes. This strategy is not available for intramolecular reactions. The latter reactions are discussed here: it is shown how relative rate considerations and/or the presence of biphasic decays can reveal the presence of additional steps that are coupled to the intramolecular electron transfer.

Single-Step Electron-Transfer Reactions

Electron transfer between two weakly interacting sites is controlled by the Franck–Condon principle.[11] Internuclear distances and nuclear velocities remain constant during an electronic transition, and as a consequence, the nuclear configuration of the system does not change during the actual electron transfer. In classical electron-transfer theory (activated complex theory is usually used[11-13]) this requires that the electron transfer occur only after the system has reorganized so that its energy is independent of the redox site on which the electron is located.

The free energy of the reactants[14] can be represented by an N-dimensional surface in an $(N + 1)$-dimensional nuclear-configuration space. There is a similar surface for the products. In general the minima of the reactant and product states occur at different nuclear configurations due to changes in bond lengths, bond angles, and solvent polarization resulting from the movement of charge from one site to another. Figure 1 shows a contour plot of the lowest energy surface for an intramolecular electron-transfer reaction in which the reactant and product states each have only a single (stable) configuration and where there are changes in the equilibrium nuclear configuration in only two nuclear coordinates, q_f and q_c, associated with a fast and a slow vibrational mode, respectively. Further, it has been assumed that the motion of the system along the nuclear coordinates is harmonic and that transferring the charge does not change the "reduced" force constants of the two modes.[15]

In the classical model the electron transfer occurs at the intersection of the energy surfaces for the reactant and product states. Within the activated-complex framework the lowest (energy) point of intersection of the two surfaces is identified as the activated complex or transition state for the reaction. The transition state is located at the intersection of the short and long dashes in Figure 1. The "fast" coordinate, q_f in Figure 1, is generally associated with the intramolecular vibrations, while the "slow" coordinate q_c is usually associated with either the collective solvent motions or a conformational motion of the reactant. The classical reaction path is the path of steepest descent from the transition state and is shown as the curved dashed line joining the reactant R and product P minima. It is calculated from eq 1,[16]

$$q_c = q_c^i + \left(\frac{q_f - q_f^i}{q_f^\ddagger - q_f^i}\right)^F (q_c^\ddagger - q_c^i) \qquad (1)$$

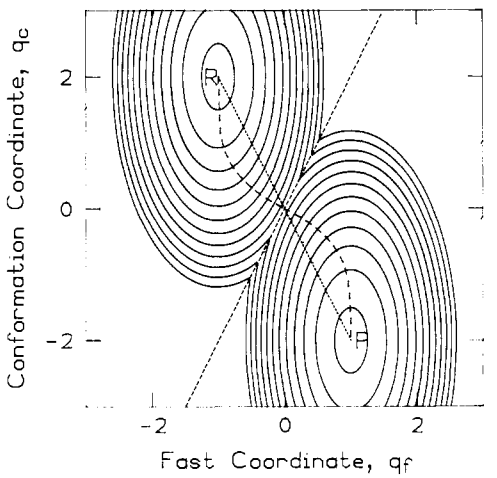

Figure 1. Contour plot of the free energy surface for the electron-transfer reaction R → P with zero driving force ($\Delta G^0_{rp} = 0$). The minimum in the reactant state R is in the upper left corner; the product minimum P is in the lower right corner. Only two coordinates contribute to the reorganization parameters, a fast coordinate q_f and a conformational coordinate q_c. The solid ellipses are the equally spaced energy contours. The long dashes show the classical reaction path for the reaction, the dotted line is the reaction coordinate, and the short dashes show the intersection of the reactant and product states. The surface is drawn assuming that $H_{rp} = 0$ (where H_{rp} is the electronic coupling matrix element between the reactant and product states), the reactants and products have identical (reduced) force constants, the ratio of the force constants for the conformational and fast coordinates is 4, and the change in the conformational coordinate between the stable reactant and product configurations is half that for the fast coordinate resulting in $\lambda_c = \lambda_f$.

where i = r or p depending on whether the reaction path is on the reactant's or product's free energy surface, $(q_f^\ddagger, q_c^\ddagger)$, (q_f^r, q_c^r), and (q_f^p, q_c^p) are the coordinates of the transition state and the equilibrium nuclear configurations of the reactants and products, respectively, and $F = f_c/f_f$, where f_f and f_c are the reduced force constants for the two modes. The reaction path is clearly *not* a straight line: initially the motion is primarily along the coordinate of the low-frequency (slow) mode, while close to the transition state the motion is mainly along the coordinate of the high-frequency (fast) mode. As the difference between the force constants for the two modes increases, the motion is almost exclusively along the low-frequency mode initially and the high-frequency mode at the transition state (i.e., the reaction path develops "corners"). However, the reaction does not proceed in two discrete steps in which first the low-frequency mode and then the high-frequency mode reorganizes. Even in the limit of very different force constants, in the one-step or concerted reaction the two modes reorganize only to a configuration that is appropriate to the transition state for the concerted reaction—this transition state is located on the straight line joining the reactant and product minima, and its energy determines the rate of the reaction. By contrast, two transition states are important in a two-step mechanism with the

(11) Sutin, N. *Annu. Rev. Nucl. Sci.* **1962**, *12*, 285–328.
(12) Marcus, R. A.; Sutin, N. *Biochim. Biophys. Acta* **1985**, *811*, 265–322.
(13) Hush, N. S. *Prog. Inorg. Chem.* **1987**, *8*, 391.
(14) The electron-transfer reactions considered in this paper are for systems in which two redox-active sites are contained within a single molecular framework and consequently the reactions are unimolecular. Strictly speaking, the reactions have only a single reactant and a single product. However, since the electron transfer occurs between two redox sites it is sometimes convenient to refer to these two sites as the reactants (or products). One should remember that the two redox sites are not able to freely diffuse together or apart.
(15) Brunschwig, B. S.; Logan, J.; Newton, M. D.; Sutin, N. *J. Am. Chem. Soc.* **1980**, *102*, 5798.

(16) The equation for the reaction path can be derived as follows. The reactant's surface is described by $V(q_f,q_c) = {}^1/_2 f_f(q_f - q_f^r)^2 + {}^1/_2 f_c(q_c - q_c^r)^2$, where q_f and q_c are the nuclear coordinates of the reactant. The gradient of V is $\vec{\nabla} V = f_f(q_f - q_f^r)\vec{i} + f_c(q_c - q_c^r)\vec{j}$, where $\vec{i}$ and $\vec{j}$ are the unit vectors in the q_f and q_c directions, respectively. Since the reaction path is defined as the path of steepest descent from the transition state, the direction of the reaction path is along the gradient of V. Thus the projection of the reaction path onto the q_f,q_c plane has a slope $m_{rp} = dq_c/dq_f = f_c(q_c - q_c^r)/f_f(q_f - q_f^r)$. Integrating this expression and using the transition-state coordinates $(q_f^\ddagger, q_c^\ddagger)$ to evaluate the constant of integration gives eq 1, where i = r. The same approach is used to derive the reaction path on the product's surface. The direction of the projection of the reaction path as a function of q_f alone can be obtained from the slope of the projection of the reaction path, m_{rp} calculated, by using eq 1. For the reactant's surface this gives $m_{rp} = F((q_f - q_f^r)/(q_f^\ddagger - q_f^r))^{F-1}(q_c^\ddagger - q_c^r)$, where $F = f_c/f_f$. As the reactant's minimum, (q_f^r, q_c^r), is approached, if $F \ll 1$, then $m_{rp} = F[(q_f^\ddagger - q_f^r)/(q_f - q_f^r)](q_c^\ddagger - q_c^r) \to \infty$, (since the denominator approaches zero), and the reaction path is oriented along the q_c direction (slow mode). Likewise at the transition state $m_{rp} \to F(q_c^\ddagger - q_c^r)$. The line has a small slope and so the reaction path is primarily oriented along the q_f direction (fast mode). Of course, when $F \gg 1$, the opposite conclusions are reached.

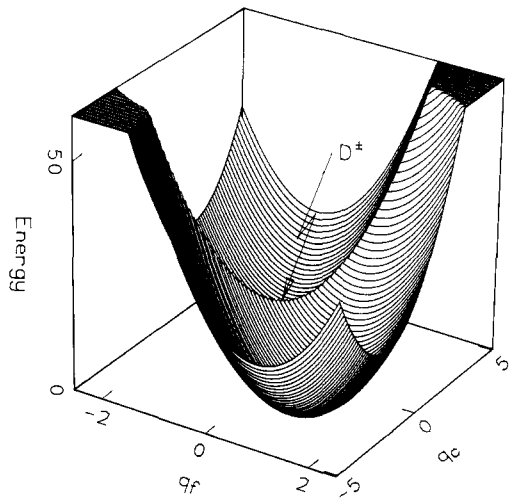

Figure 2. Three-dimensional representation of the free energy surface shown in Figure 1. The surface is oriented so that the minimum in the product state is toward the right front of the figure. The reactant minimum is toward the left rear of the figure and is obscured by the surface. The transition state is the point marked $D^{\pm}$. The line of intersection of the reactant and product states shown in Figure 1 is the ridge line that runs from front left to right rear. The surface is drawn by using the same parameters as in Figure 1.

overall rate of the reaction depending on the energies of these two states.

The short dashes in Figure 1 define the "line" of intersection of the reactants' and products' energy surfaces. The projection of this line has a slope ($\Delta q_c/\Delta q_f$) and intercept (q_c value at q_f = 0) given by

$$\text{slope} = \frac{f_f(q_f^p - q_f^r)}{f_c(q_c^r - q_c^p)} \tag{2a}$$

$$\text{intercept} = \frac{q_c^r + q_c^p}{2} + \frac{f_f(q_f^{r\,2} - q_f^{p\,2})}{f_c(q_c^r - q_c^p)} - \frac{\Delta G^0_{rp}}{2f_c(q_c^r - q_c^p)} \tag{2b}$$

(The projection of the line of intersection is not a straight line when the force constants for the two surfaces differ but will curve at large values (positive or negative) of q_c. This curvature is dependent on the ratio of the force constants for a particular mode in the reactant and product states. Further, the symmetry of the contour map is lost with the nuclear configuration of the activated complex no longer lying on the straight line joining the two minima.[15])

A three-dimensional representation of the energy surface considered above is shown in Figure 2. The product minimum is in the foreground, the ridge line[17] is the line of intersection of the reactant and product states, and $D^{\pm}$, the minimum in this ridge line, is the transition state. A plot of the free energy of the reactant and product states as a function of the reaction coordinate is shown in Figure 3, where again the reactant's and product's profiles are harmonic with identical (reduced) force constants, ΔG^*_{rp} is the activation free energy, and $2H_{rp}$ is the splitting between the two surfaces.[11] The reaction coordinate is the straight line connecting the projections of the minima of the reactant and product states in Figure 1.[18,19] Figure 3 is obtained by taking a cut through the surfaces shown in Figure 1 along the reaction coordinate.

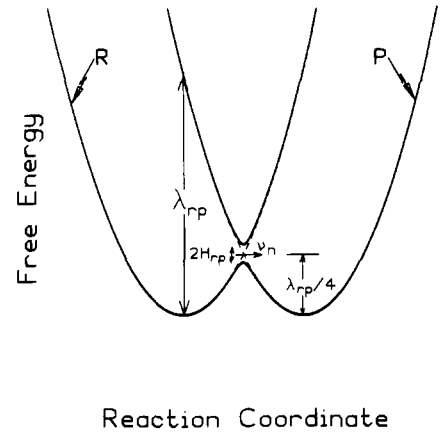

Figure 3. Plot of the free energy of the reactant (left curve) and product (right curve) states as a function of the reaction coordinate (nuclear configuration). The splitting at the intersection is equal to $2H_{rp}$, where H_{rp} is the electronic coupling matrix element. The reorganization parameter λ_{rp} is the difference between the energies of the reactant and product states at the reactant's equilibrium nuclear configuration (minimum), and ν_n is the frequency of the nuclear motion that takes the system over the barrier. The transition state is located at the intersection of the two curves. The figure is drawn by using the same parameters as in Figure 1.

In the semiclassical theory[11,15,20] the rate constant for a (first-order) electron-transfer reaction is given by

$$k_{rp} = \kappa_{el}\nu_n\Gamma_n e^{-\Delta G^*_{rp}/RT} \tag{3}$$

$$\Delta G^*_{rp} = \frac{(\lambda_{rp} + \Delta G^0_{rp})^2}{4\lambda_{rp}} \tag{4}$$

$$\kappa_{el} = \frac{2\pi H_{rp}^2}{h\nu_n}\left(\frac{\pi}{\lambda_{rp}RT}\right)^{1/2} \tag{5}$$

where κ_{el} is the nonadiabaticity factor,[21] ν_n is the frequency of the nuclear motion that takes the system over the barrier, Γ_n is the correction for nuclear tunneling, ΔG^0_{rp} is the overall free energy change, and λ_{rp} is the reorganization parameter for the reaction. The reorganization parameter is the difference between the energies of the reactants and products at the equilibrium nuclear configuration of the reactants for the case where $\Delta G^0_{rp} = 0$ (see Figure 3). λ_{rp} is the sum of contributions from each nuclear coordinate undergoing a displacement during the reaction. In the present context two contributions to λ_{rp} are considered: one, λ_c, is associated with a particular (slow) conformation change within the reactant (in an analogous treatment of slow solvent reorganization, λ_c could be identified with the solvent reorganization) and the other, λ_f, with the remaining (fast) contributions to the reorganization parameter.

Although ν_n is often set equal to kT/h, the prefactor in transition-state expressions, a better approximation is to use a reorganization-energy weighted average of the frequencies for the nuclear coordinates contributing to the activation barrier.[22] In this case ν_n is approximately equal to the fastest vibrational frequency associated with a nuclear coordinate that contributes to λ.[22] For electron-transfer reactions that are faster than the slowest nuclear reorganization it has been suggested that the frequency factor should reflect the dynamical properties of the solvent.[23-28]

(17) The roughness in the ridge line is an artifact of the plotting software.

(18) The reaction coordinate should not be confused with the reaction path discussed above.[19] The reaction path is the path of steepest descent from the top of the (potential) barrier and is determined by the actual dynamics of the reaction. In the systems considered here, the reaction coordinate is a straight line connecting the projections of the minima of the energy surfaces; in general, the reaction coordinate is generated by the projection of the saddle point as the energy of the basin representing the products is displaced vertically.

(19) Sutin, N.; Brunschwig, B. S.; Creutz, C.; Fujita, E.; Winkler, J. R. In Proceedings of Eleventh DOE Solar Photochemistry Research Conference. National Technical Information Service: LBL-23453, Tahoe City, CA, 1987; pp 105-110.

(20) Brunschwig, B. S.; Sutin, N. *Comments Inorg. Chem.* **1987**, *6*, 209-235.

(21) $\kappa_{el} \approx 1$ when the reaction is adiabatic and $\ll 1$ for very nonadiabatic reactions.[12,15]

(22) Sutin, N.; Brunschwig, B. S. *ACS Symp. Ser.* **1982**, *198*, 105-135.

(23) Sumi, H.; Marcus, R. A. *J. Chem. Phys.* **1986**, *84*, 4272-4276.

(24) Sumi, H.; Marcus, R. A. *J. Chem. Phys.* **1986**, *84*, 4894-4914.

(25) Nadler, W.; Marcus, R. A. *J. Chem. Phys.* **1987**, *86*, 3906-3924.

(26) Nadler, W.; Marcus, R. A. *Chem. Phys. Lett.* **1988**, *144*, 24-30.

(27) Rips, I.; Klafter, J.; Jortner, J. *J. Chem. Phys.* **1988**, *89*, 4288-4299.

(28) van der Zwan, G.; Hynes, J. T. *J. Chem. Phys.* **1982**, *76*, 2993-3001. van der Zwan, G.; Hynes, J. T. *J. Phys. Chem.* **1985**, *89*, 4181-4188. Hynes, J. T. *J. Phys. Chem.* **1986**, *90*, 3701-3706.

Table I. Observed Rate Constants for Direct and Two-Step Reactions

mechanism	case 1a	case 1b	case 2
$R \rightarrow P$	k_{rp}		
$R \rightleftharpoons R^* \rightleftharpoons P$		$K_{rr^*}k_{r^*p}$ [$k_{r^*r} \gg k_{rr^*}, k_{r^*p}, k_{pr^*}$]	k_{rr^*} [$k_{r^*p} \gg k_{rr^*}, k_{r^*r}, k_{pr^*}$]
$R \rightleftharpoons P^* \rightleftharpoons P$	k_{rp^*} [$k_{rp^*} \gg k_{p^*r}, k_{p^*p}, k_{pp^*}$]	$K_{rp^*}k_{p^*p}$ [$k_{p^*r} \gg k_{rp^*}, k_{p^*p}, k_{pp^*}$]	k_{rp^*} [$k_{p^*p} \gg k_{rp^*}, k_{p^*r}, k_{pp^*}$]

However for these very fast reactions simple activated-complex theory is no longer applicable, and the problem must be reformulated. One such situation can still be considered by using activated-complex theory; namely, the case where the electron-transfer reaction is so fast that the slow nuclear coordinates effectively remain frozen.[29] The reaction can then be formulated as a two-step process.

Two-Step Electron-Transfer Reactions

The rates of single-step electron-transfer reactions depend upon λ_{rp} and H_{rp} (eq 3–5). When λ_{rp} is large or H_{rp} is very small, the direct reaction will be slow and a more complicated mechanism may operate. Such a situation may obtain when the electron transfer is subject to spin-multiplicity restrictions.[30–32] For macromolecular systems several conformations of the reactant and product may be thermally accessible, and some of these conformers may have much more favorable electron-transfer properties than those of the stable reactant or product.

The present discussion will focus on two types of mechanisms. In the first, an unstable conformer R* of the reactant is formed prior to the electron transfer. The two conformers R and R* have different nuclear configurations and electronic structures, and consequently the reaction involving R* will generally have κ_{el}, λ_{r^*p}, and $\Delta G^0_{r^*p}$ values that differ from those of the reaction involving R. To focus on the effects due to nuclear-configuration changes, we assume that κ_{el} is the same for the reactions involving R or R* (i.e., $H_{rp} = H_{r^*p}$). In the second type of mechanism, electron transfer yields an unstable product conformer P*. Again P* and P have different nuclear configurations and electronic structures, and we assume that $H_{rp} = H_{rp^*}$.

Scheme I summarizes the two-step mechanisms considered above and, in addition, allows for the possibility of slow rate-determining conformation changes. In this scheme $K_{rr^*} = k_{rr^*}/k_{r^*r}$

Scheme I

$$R \underset{k_{r^*r}}{\overset{k_{rr^*}}{\rightleftharpoons}} R^* \underset{k_{pr^*}}{\overset{k_{r^*p}}{\rightleftharpoons}} P \qquad (6)$$

$$R \underset{k_{p^*r}}{\overset{k_{rp^*}}{\rightleftharpoons}} P^* \underset{k_{pp^*}}{\overset{k_{p^*p}}{\rightleftharpoons}} P \qquad (7)$$

and $K_{pp^*} = k_{pp^*}/k_{p^*p}$ are the equilibrium constants for the conformation changes, K_{rp} is the equilibrium constant for the overall reaction, k_{r^*p} and k_{rp^*} are the rate constants for the forward and k_{pr^*} and k_{p^*r} those for the reverse electron transfers, respectively. The spectra of the stable and unstable conformers are assumed to be similar so that their interconversion cannot be observed directly.[33] Equations 6 and 7 are of the same general form and their kinetics are treated in the Appendix. The term "gating" will be used to describe the situation where the observed rate is controlled by a slow conformational change.

Two limiting cases are important. Case 1 applies when the first step of the reaction is much faster than the second step, while case 2 applies when the opposite is true. Case 1 is further subdivided depending on whether the forward (case 1a) or the reverse (case 1b) rate constant of the first step is larger. Table I summarizes the observed rate constants in the various regimes (see the Appendix for details).

For the R* mechanism, only the conversion of R + R* to P can be observed. Since R is the dominant reactant form, case 1a (which assumes $k_{rr^*} > k_{r^*r}$) is not applicable. In case 1b a slow rate-controlling electron-transfer step k_{r^*p} is preceded by a fast conformational preequilibrium, while in case 2 the reaction is gated and the rate constant for the slow conformation change controls the observed rate of formation of P. For the P* mechanism the observed reaction is the conversion of R to P* + P. When either the forward electron-transfer rate constant (case 1a) or the conformational rate constants (case 2) are the largest, the observed rate constant is that of the forward electron-transfer step k_{rp^*}. The observed kinetics are independent of the subsequent conversion of P* to P (it is slow for case 1a, i.e., there is a buildup of P*, and fast for case 2). When the back electron-transfer rate constant is largest, case 1b, the usual preequilibrium rate expression applies and the observed rate constant reflects both the conformational and electron-transfer steps. The kinetics are controlled by the conformation change and the reaction is gated. Case 1b applies only when the $R \rightarrow P^*$ reaction is energetically unfavorable (i.e., $\Delta G^0_{pp^*} > -\Delta G^0_{rp}$, where $\Delta G^0_{pp^*}$ is the free energy change for $P \rightarrow P^*$). Biexponential decay will be observed in case 1 when the forward and back electron-transfer rate constants are comparable ($\Delta G^0_{pp^*} \approx -\Delta G^0_{rp}$). The time constants for the two decays are given in the Appendix.

The observed rate will, of course, reflect only the two-step mechanism when the latter is faster than the direct reaction. Note that only in case 2 of the R* mechanism and case 1b of the P* mechanism are the reactions gated. The next section will consider the conditions under which the two-step mechanisms are favorable.

Two-Step versus Direct Mechanisms

In forming R* one (or more) of the nuclear coordinates of the reactant has changed. We assume that the equilibrium nuclear configurations of R* and R differ in only a single coordinate. When this coordinate is q_c, a coordinate that is "active" in the $R \rightarrow P$ electron-transfer reaction (i.e., it has different equilibrium values for R and P), then P may be more similar to R* than to R (i.e., $|q_c^{r^*} - q_c^p| < |q_c^r - q_c^p|$). This type of R* conformer will be referred to as a low-λ intermediate since the reorganization parameter λ_{r^*p} for the electron-transfer reaction of the unstable conformer ($R^* \rightarrow P$) is *smaller* than that for the direct reaction[34] ($\lambda_{r^*p} < \lambda_{rp}$). When the nuclear coordinate that undergoes change in the formation of R* is an electron-transfer "inactive" coordinate, then P will be more similar to R than to R* (i.e., $|q^{r^*} - q^p| > |q^r - q^p|$, where $q^r = q^p$). The R* conformer resembles P less than

(29) The reaction path in this case will proceed from the reactant's minimum parallel to the q_f axis (i.e., initially only q_f will change). Only after crossing the barrier will the path begin to curve with both q_f and q_c changing. The free energy barrier is larger than the value calculated from eq 2 since both λ_{rp} and ΔG^0_{rp} need to be modified. The correct expressions are $\lambda' = \lambda_f$, $\Delta G^{0\prime} = \Delta G^0_{rp} + \lambda_c$, and $\Delta G^{*\prime} = (\Delta G^0_{rp} + \lambda_c + \lambda_f)^2/(4\lambda_f)$, where the primed terms are those appropriate to the fast reaction and the unprimed those of the overall reaction.

(30) In 1951 it was recognized[31] that, due to so-called "spin restrictions", the H_{rp} for the self-exchange reaction of $Co(NH_3)_6^{2+/3+}$ would be very small. The $Co(NH_3)_6^{2+}$ has a high-spin ground electronic state ($t_{2g}^5e_g^2$), while the $Co(NH_3)_6^{3+}$ has a low-spin ground state (t_{2g}^6) due to the larger ligand field splitting of the cobalt(III) complex. Due to the small H_{rp} it was suggested that the reaction may proceed by a preequilibrium involving the low-spin excited electronic state of the Co(II) species. In this case it was expected that the κ_{el} for the two-step pathway would be much more favorable.

(31) Friedman, H. L.; Hunt, J. P.; Plane, R. A.; Taube, H. *J. Am. Chem. Soc.* **1951**, *73*, 4028.

(32) Winkler, J. R.; Rice, S. F.; Gray, H. B. *Comments Inorg. Chem.* **1981**, *1*, 47–51.

(33) Since $K_{rr^*} \ll 1$ and therefore only very small amounts of R* are ever present, the assumption regarding the similarity of the spectra of the stable and unstable conformers can be relaxed for the R* mechanism.

(34) The reorganization parameter for an electron-transfer reaction is related to both the change in the equilibrium nuclear configuration ($q_i^r - q_i^p$) and to the "reduced" force constant for that coordinate f_{q_i}. Since the various energy surfaces are assumed to be harmonic, the reorganization parameter for that coordinate is $\lambda_i = f_{q_i}(q_i^r - q_i^p)^2/2$, where the coordinates and force constants are those for the normal-mode motion. Therefore, when the reorganization parameters for two different reactions ($R \rightarrow P$ and $R^* \rightarrow P$) are compared, both the force constants and the changes in the nuclear configuration need to be considered. The force constant are assumed to be equal for the energy surfaces considered here, and consequently only the configuration changes need to be compared: the reaction with the larger configuration change will have the larger reorganization parameter.

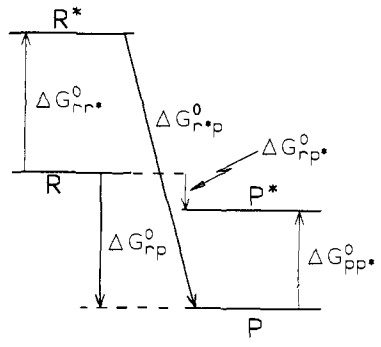

Figure 4. Illustration of the free-energy relationships between the two conformers of the reactant and product. ΔG^0_{rp} is the overall free energy change for the reaction, ΔG^0_{rr*} and ΔG^0_{pp*} are the free energies of the unstable conformers relative to that of the stable conformer for the reactant and product, respectively, and ΔG^0_{r*p} and ΔG^0_{rp*} are the free energy changes for the reactions R* → P and R → P*, respectively.

R does and will be designated a high-λ intermediate since in this case the reorganization parameter for the electron-transfer reaction of the unstable conformer is *larger* than that for the direct reaction[34] ($\lambda_{r*p} > \lambda_{rp}$). An analogous description applies to product conformers. We first compare reactions involving low-λ intermediates with the corresponding direct reactions. Then reactions involving high-λ intermediates will be considered. Applications utilizing low- or high-λ intermediates are explored in the last section.

Low-λ Intermediates. Although the equilibrium configurations of R and P occur at different values of the q_f and q_c coordinates, for the R* mechanism we assume that the equilibrium value of the q_c coordinate of R* is the same as that for P. In other words, the equilibrium nuclear configurations of R and R* are (q_f^r, q_c^r) and (q_f^r, q_c^p), respectively, and $\lambda_{r*p} = \lambda_f$. For the P* mechanism we also assume that the equilibrium nuclear configurations of P* and P are (q_f^p, q_c^p) and (q_f^p, q_c^r), respectively, differing only in the q_c coordinate. The equilibrium nuclear configurations of R, P*, P, and R* lie at the corners of a rectangle.

The energy relationships between the various species are shown in Figure 4, where ΔG^0_{rr*} and ΔG^0_{pp*} are the free energy change for R → R* and P → P*, respectively, and ΔG^0_{r*p} and ΔG^0_{rp*} are the changes for the electron-transfer reactions R* → P and R → P*, respectively. ΔG^0_{rp} is negative—the overall reaction is favorable, and ΔG^0_{rr*} and ΔG^0_{pp*} are always positive. The various free energies are related by eq 8 and 9.

$$\Delta G^0_{rp} = \Delta G^0_{rr*} + \Delta G^0_{r*p} \quad (8)$$

$$\Delta G^0_{rp} = \Delta G^0_{rp*} - \Delta G^0_{pp*} \quad (9)$$

Unstabilized Low-λ Intermediates. The energetics of the two-step and direct mechanisms are most readily compared by considering the free energy surface upon which the reactions occur. We assume that the electron-transfer rate constants can be expressed in terms of eq 3–5, that the (reduced) force constants for the two modes do not change either during the conformation changes or in the electron-transfer reaction, and that the energy surfaces are harmonic.

Consider case 1b (the preequilibrium case) for the R* mechanism (eq 6) and assume that $\Delta G^0_{rr*} = \lambda_c$ where $K_{rr*} = \exp[-\lambda_c/RT]$. Figure 5 shows the surfaces for $\Delta G^0_{rr*} = \Delta G^0_{pp*} = \lambda_c$. In both Figure 5a and 5b the direct reaction has the lowest energy transition state (activation barrier). The activation barriers for the direct and two-step pathways can also be compared analytically. From Table I the observed rate constant for the *R** mechanism is equal to $K_{rr*}k_{r*p}$. The free energy barrier for the k_{r*p} step, measured relative to the energy minimum of R*, is

$$\Delta G^*_{r*p} = [\lambda_f + (\Delta G^0_{rp} - \lambda_c)]^2/4\lambda_f \quad (10)$$

where $\Delta G^0_{rp} - \lambda_c$ is the free energy change and λ_f is the reorganization parameter for the electron-transfer step. The R* → P barrier is lower than that for the direct reaction. However, the barrier relative to R is that of the electron-transfer step plus the energy of the R* minimum. It is easily shown (eq 11) that for this case the total barrier for the preequilibrium mechanism is always *larger* than that for the direct k_{rp} path

$$\lambda_c + \frac{(\Delta G^0_{rp} - \lambda_c + \lambda_f)^2}{4\lambda_f} \geq \frac{(\Delta G^0_{rp} + \lambda_{rp})^2}{4\lambda_f} + \frac{\lambda_c|\Delta G^0_{rp}|}{2\lambda_f} > \frac{(\Delta G^0_{rp} + \lambda_{rp})^2}{4\lambda_{rp}} \quad (11)$$

where $\lambda_{rp} = \lambda_c + \lambda_f$. In other words, the direct electron transfer

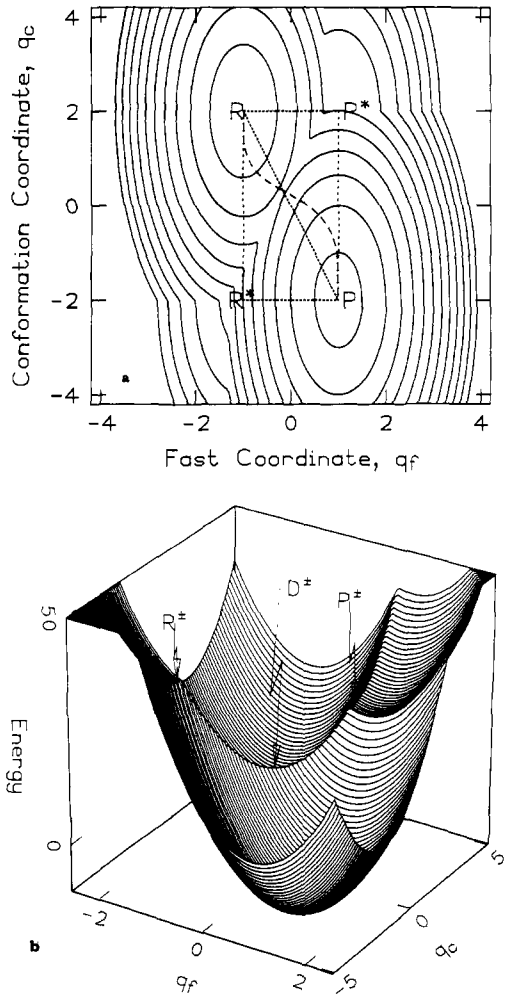

Figure 5. (a) Contour plot of the free energy surface for an electron-transfer reaction in which the reactant and product each have a low-λ unstable conformer. The stable reactant and stable product minima are labeled R and P, respectively, while R* and P* indicate the minima of the unstable reactant and product conformers. Both unstable conformers have an energy of λ_c relative to their stable forms. The dashed line is the reaction path for the direct reaction R → P, and the dotted line that connects the R and P minima is the reaction coordinate for this reaction. The transition state for this direct reaction is at the intersection of these two lines. The widely spaced dotted lines show the reaction coordinate for the conformation changes while the closely spaced dotted lines that connect R* to P and R to P* are the reaction coordinate for the electron-transfer reactions R* → P and R → P*, respectively. The surface is drawn assuming that $\Delta G^0_{rp} = 0.15\lambda_{rp}$, $H_{rp} = 0$, the reactant and product have identical (reduced) force constants, the ratio of the force constants for the conformational and fast coordinates is 4, and the change in the conformational coordinate between the reactant's and product's minima is half that for the fast coordinate resulting in $\lambda_c = \lambda_f$. (b) Three-dimensional representation of the free energy surface shown in Figure 5a. The product surface is located closest to the observer, the reactant surface is located toward the rear left: P* is located to the rear right and R* is to the front left. The transition states for the reactions R → P, R* → P, and R → P* are indicated by $D^{\pm}$, $R^{\pm}$, and $P^{\pm}$, respectively: $D^{\pm}$ has the lowest energy.

Table II. Free-Energy Barriers (ΔG^*) for Direct and Two-Step Electron-Transfer Reactions with Low-λ Intermediates

mechanism	case 1a	case 1b	case 2
$R \rightarrow P$	$(\Delta G^0_{rp} + \lambda_c + \lambda_f)^2/[4(\lambda_c + \lambda_f)]$		
$R \rightleftharpoons R^* \rightleftharpoons P$		$\Delta G^0_{rr^*} + (\Delta G^0_{rp} - \Delta G^0_{rr^*} + \lambda_f)^2/(4\lambda_f)$	$(\Delta G^0_{rr^*} + \lambda_c)^2/(4\lambda_c)$
$R \rightleftharpoons P^* \rightleftharpoons P$	$(\Delta G^0_{rp} + \Delta G^0_{pp^*} + \lambda_f)^2/(4\lambda_f)$	$\Delta G^0_{rp^*} + (-\Delta G^0_{pp^*} + \lambda_c)^2/(4\lambda_c)$	$(\Delta G^0_{rp} + \Delta G^0_{pp^*} + \lambda_f)^2/(4\lambda_f)$

is energetically more favorable in this case as was observed in Figure 5. In the direct electron-transfer reaction the transition-state energy is normally only a fraction of the total reorganization parameter,[35] while the value of q_c at the transition state is intermediate between its values in the reactant's and product's equilibrium configurations. For case 1b the total energy of the preequilibrium contributes to the overall reaction barrier since the value of the conformation coordinate at the $R^* \rightarrow P$ transition state is fully that of the stable product. This contribution to the energy (for $K_{rr^*} = \exp(-\lambda_c/RT)$) more than cancels the reduction in the barrier for the electron-transfer step due to the smaller reorganization parameter. Even though R* has more favorable kinetic properties than R, its low equilibrium concentration decreases its effectiveness in the reaction.

In the P* mechanism, electron transfer yields an unstable product P*. The activation free energy for the electron-transfer step ($R \rightarrow P^*$) is

$$\Delta G^*_{rp^*} = (\lambda_f + \Delta G^0_{rp^*})^2/4\lambda_f \qquad (12)$$

where $\Delta G^0_{rp^*}$ is the free energy change for this step. When the energy of P* (relative to P) is λ_c then the electron-transfer barrier (and therefore also the total barrier if case 1a or 2 applies) for the two-step mechanism is again larger than that for direct reaction (eq 13):

$$\Delta G^*_{rp^*} = \frac{[\lambda_f + (\Delta G^0_{rp} + \lambda_c)]^2}{4\lambda_f} = \frac{(\lambda_{rp} + \Delta G^0_{rp})^2}{4\lambda_f} > \frac{(\lambda_{rp} + \Delta G^0_{rp})^2}{4\lambda_{rp}} \qquad (13)$$

Stabilized Low-λ Intermediates. The above considerations show that the two-step mechanisms are not necessarily more favorable than the direct, concerted mechanism. This conclusion differs from that stated in ref 10.[36] For the two-step pathway to be faster than the direct reaction, the intermediate needs to be stabilized. Thus, while a two-step mechanism is not energetically favored when R* or P* has an energy of λ_c relative to the stable conformer, such a mechanism becomes more favorable as the energy of the intermediate is lowered.

The free-energy surface for the case where the two intermediates are only slightly less stable than either the reactant or the product is shown in Figure 6. It is readily apparent that the transition state for the direct reaction has a higher energy than the transition states for the two-step mechanisms. It is also evident that the transition states for the two-step mechanisms have different energies. This is seen analytically for the R* mechanism with $\Delta G^0_{rr^*} \approx 0$ and $\Delta G^0_{rp} \approx 0$. The activation barrier for the two-step mechanism is just that of the electron-transfer step, $\lambda_f/4$ (since $K_{rr^*} \approx 1$, the fast conformation change contributes a factor of only 0.5 to the rate). The barrier for the direct reaction is $\lambda_{rp}/4$, and consequently the two-step mechanism has the lower barrier. The two-step mechanism is, therefore, energetically favored in the limit of a very highly stabilized R* intermediate.[37] An analogous situation is also found for the P* mechanism.

Low-λ Intermediates: Normal Region. A free-energy surface for the three mechanisms is shown in Figure 7, where the transition

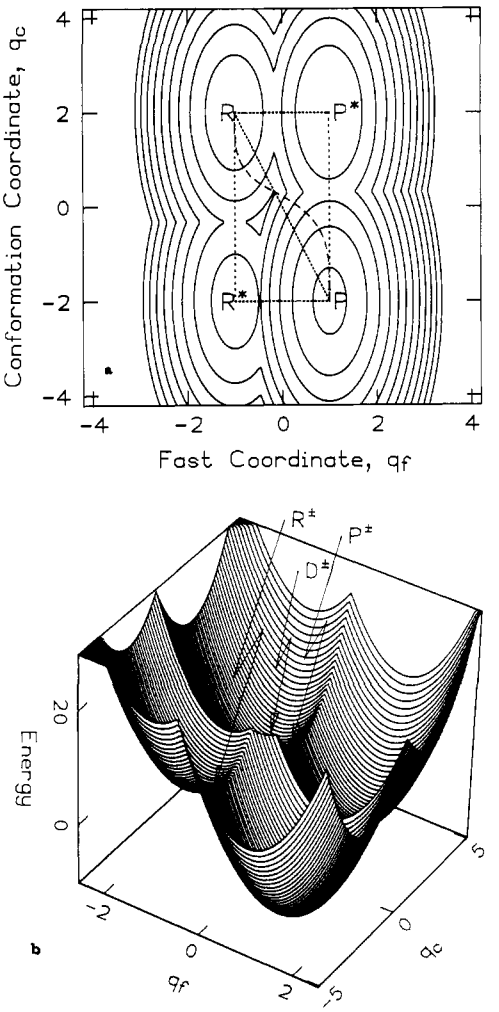

Figure 6. (a) Contour plot of the free energy surface for an electron-transfer reaction in which the reactant and product each have a low-λ unstable conformer. The parameters are the same as in Figure 5a except that the energies of the unstable conformers are $\Delta G^0_{rr^*} = \Delta G^0_{pp^*} = 0.16\lambda_c = 5$ energy units. (b) Three-dimensional representation of the free energy surface shown in Figure 6a. The orientation of the surface is the same as in Figure 5b. The transition states $R^{\pm}$ and $P^{\pm}$ are both lower in energy than $D^{\pm}$.

states for the direct and two-step mechanisms have similar energies. This case is intermediate to those considered in Figures 5 and 6. Figure 7 reveals that the barrier for k_{p^*p} is larger than the barrier for k_{p^*r}.[38] The expressions for the free energy barriers for the direct and the two-step pathways are summarized in Table II.

The barriers for the electron-transfer steps are calculated from eq 4 with the reorganization parameters and driving forces appropriate to the particular step. The barriers for the conformation changes are calculated in an analogous manner. The expression

(35) For reactions that have zero driving force the activation barrier is equal to $\lambda/4$.

(36) Actually ref 10 is somewhat ambiguous on this point. Although the authors do refer to stable conformational intermediates, they also assert that, for systems such as shown in Scheme II, the two-step mechanism will always proceed faster than the concerted reaction.

(37) This statement is true only in the normal region; for highly exergonic reactions the reaction with the larger reorganization parameter is favored.

(38) It is also necessary to consider the prefactors for the reactions. For the electron-transfer case the prefactor is $\kappa_{el}\nu_n \leq \nu_n$, while for the conformation change the prefactor is just the nuclear vibration frequency associated with the conformation change. When the dominant nuclear reorganizations are for the conformation change, it is expected that the two frequencies will have similar magnitudes. However, when the conformation change is very slow or there is a significant contribution from a high-frequency mode to the electron-transfer barrier, then the two prefactors could be different. In this latter case the prefactor may favor the electron transfer and case 1 may be relevant.

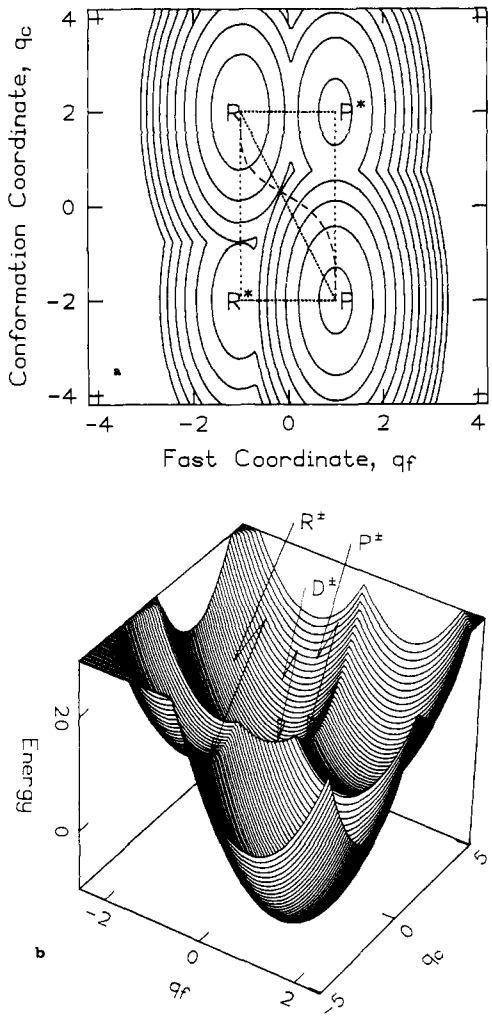

Figure 7. (a) Contour plot of the free energy surface for an electron-transfer reaction in which the reactant and product each have a low-λ unstable conformer. The parameters are the same as in Figure 4a except that the energies of the unstable conformers are $\Delta G^0_{rr^*} = \Delta G^0_{pp^*} = \lambda_c/3 = 11$ energy units. (b) Three-dimensional representation of the free energy surface shown in Figure 7a. The orientation of the surface is the same as in Figure 4b. The transition states R‡, P‡, and D‡ are all close in energy.

for the barrier in the case of a preequilibrium step preceding the electron-transfer reaction, R* mechanism, case 1b, reveals two opposing trends. The barrier for the electron-transfer step is lowered due to both the smaller reorganization parameter (λ_f rather than $\lambda_c + \lambda_f$) and the increase in the driving force by $\Delta G^0_{rr^*}$;[39] on the other hand, the energy of the unfavorable preequilibrium, $\Delta G^0_{rr^*}$, increases the total effective barrier to the reaction. This mechanism is favored by large λ_f, which ensures that $(\Delta G^0_{rp} - \Delta G^0_f + \lambda_f) \geq 0$, and by small $\Delta G^0_{rr^*}$. For the P* mechanism (case 2) the opposing trends are also evident. Here the reorganization parameter in the electron-transfer step has also decreased by λ_c; however, the free-energy change has been made less favorable by $\Delta G^0_{pp^*}$. Thus in both cases the two-step mechanism is favored by large λ_f and small $\Delta G^0_{rr^*}$ or $\Delta G^0_{pp^*}$.

Comparison of the expressions for the activation barriers for the two-step and direct mechanisms allows one to predict which mechanism will be more favorable under a given set of conditions. The equations can be solved to give expressions for the energies of R* and P*, $\Delta G^{\ddagger}_{rr^*}$ and $\Delta G^{\ddagger}_{pp^*}$, respectively, at which the two-step and the direct mechanisms have the same rates. The expressions for reaction via R* and P* are

$$\frac{\Delta G^{\ddagger}_{rr^*}}{\lambda_c} = \left(\frac{1 \pm \rho^{1/2}}{|\rho - 1|}\right)\frac{\Delta G^0_{rp}}{\lambda_{rp}} - \frac{\rho \pm \rho^{1/2}}{|\rho - 1|} \quad (14)$$

$$\frac{\Delta G^{\ddagger}_{pp^*}}{\lambda_c} = -\left(\frac{1 \pm \rho^{1/2}}{|\rho - 1|}\right)\frac{\Delta G^0_{rp}}{\lambda_{rp}} - \frac{\rho \pm \rho^{1/2}}{|\rho - 1|} \quad (15)$$

$$\rho = \frac{\lambda_{r^*p}}{\lambda_{rp}} \quad \text{or} \quad \frac{\lambda_{rp^*}}{\lambda_{rp}} = \frac{\lambda_f}{\lambda_c + \lambda_f} \leq 1 \quad (16)$$

The two-step mechanisms are favored when the energy of the intermediate, $\Delta G^0_{rr^*}$ or $\Delta G^0_{pp^*}$, falls in the range between the two solutions for $\Delta G^{\ddagger}_{rr^*}$ or $\Delta G^{\ddagger}_{pp^*}$ given above:

$$0 \leq \Delta G^{+}_i < \Delta G^0_i < \Delta G^{-}_i \quad (17)$$

where i stands for either rr* or pp*, and the appropriate roots of eq 14 or 15 are used, with all values less than zero discarded. The $\Delta G^{+}_{rr^*}$ root is set equal to zero since eq 14 yields negative values for reactions with a positive driving force.

Equations 14 and 15 are written to emphasize the linear dependence of $\Delta G^{\ddagger}_i/\lambda_c$ on $\Delta G^0_{rp}/\lambda_{rp}$. The intercepts (at $\Delta G^0_{rp}/\lambda_{rp} = 0$) of the lines are the same for the R* and P* pathways with the negative roots giving positive values for $\Delta G^{-}_i/\lambda_c$. The intercepts for the positive roots are negative. The R* and P* lines have opposite slopes with the values for $\Delta G^{-}_{rr^*}/\lambda_c$ decreasing as $\Delta G^0_{rp}/\lambda_{rp}$ becomes more negative, while $\Delta G^{\ddagger}_{pp^*}/\lambda_c$ values increase. The "x" intercept (at $\Delta G^{\ddagger}_{rr^*}/\lambda_c$ or $\Delta G^{\ddagger}_{pp^*}/\lambda_c = 0$) is $\rho^{1/2}$ for $\Delta G^{+}_{rr^*}$ and $\Delta G^{-}_{pp^*}$ and $-\rho^{1/2}$ for $\Delta G^{-}_{rr^*}$ and $\Delta G^{+}_{pp^*}$. Values of $\Delta G^{\ddagger}_{rr^*}/\lambda_c$ (short dashed lines) and $\Delta G^{\ddagger}_{pp^*}$ (long dashed lines) are plotted vs $\Delta G^0_{rp}/\lambda_{rp}$ in Figure 8. The area between the long dashed lines (the total shaded area) is the region where the P* mechanism is favored; the R* mechanism is favored in the region between the short dashed lines (the shaded area of closely spaced lines). For all other regions the direct path has the lowest energy barrier. Figure 8 shows that the R* pathway is favored only at low driving force and for $\Delta G^0_{rr^*} < \lambda_c/2$ while the P* pathway is favored over a much wider range of $\Delta G^0_{rp}/\lambda_{rp}$ and $\Delta G^0_{pp^*}$ values. When λ_c becomes the dominant contribution to the reorganization parameter, $\rho \rightarrow 0$, λ_f/λ_c decreases, the intercept approaches zero and the area where the R* mechanism is favored disappears. On the other hand, as $\rho \rightarrow 1$ (λ_f/λ_c increases), λ_f becomes the dominant contribution to λ_{rp}, the intercept $\rightarrow {}^1/_2$, and the region where the two-step mechanisms are favored (the shaded area) becomes larger. Thus small values of ρ (i.e., $\lambda_c \gg \lambda_f$ and $\lambda_{rp} \approx \lambda_c$) favor the direct reaction, while values of ρ close to 1 (i.e., $\lambda_c \ll \lambda_f$ and $\lambda_{rp} \approx \lambda_f$) favor the two-step mechanism. However, when $\rho \approx 1$ the increase in rate for the two-step mechanism is only modest since, although the conformation contribution λ_c is reduced, the reaction barrier is due primarily to λ_f. For reactions with only a small driving force, the energy of the unstable product conformer must be less than $\lambda_c/2$ for the two-step pathway to be energetically favorable. Conversely, if P* (or R*) is only slightly less stable than P (or R), then the unstable conformer should be observable. Thus there are severe constraints on the energy of P* and R* in systems where K_{pp^*} or $K_{rr^*} \ll 1$.

Low-λ Intermediates: Inverted Region. In the inverted region ($|\Delta G^0_{rp}| > \lambda_{rp}$) the direct pathway is always more favorable than the R* pathway. The driving force for the R* → P reaction is larger than that for the direct electron-transfer reaction ($|\Delta G^0_{r^*p}| > |\Delta G^0_{rp}|$), and the reorganization parameter is smaller ($\lambda_c < \lambda_c + \lambda_f$). Thus the electron-transfer step in the R* pathway is more inverted than in the direct reaction (i.e., $|\Delta G^0_{r^*p} + \lambda_c| > |\Delta G^0_{rp} + \lambda_c + \lambda_f|$). For the P* pathway, the driving force and the reorganization parameter for the electron transfer are both smaller than for the direct reaction. The driving force for the R → P* reaction is reduced by $\Delta G^0_{pp^*}$ (see Table II, case 1a). The lower driving force reduces the barrier by making the reaction less inverted (or even normal), while the lower reorganization parameter increases the barrier by making the reaction more inverted. Equations 14–16 can again be used to predict when the

(39) The increase in driving force will increase the rate only when the electron-transfer step is in the normal region (i.e., $\Delta G^0_{rp} - \Delta G^0_{rr^*} + \lambda_f > 0$). When this is not the case, an increase in driving force will decrease the rate of the overall reaction.

Table III. Free-Energy Barriers (ΔG^*) for Direct and Two-Step Electron-Transfer Reactions with High-λ Intermediates

mechanism	case 1a	case 1b	case 2
$R \rightarrow P$	$(\Delta G^0_{rp} + \lambda_f)^2/(4\lambda_f)$		
$R \rightleftharpoons R^* \rightleftharpoons P$		$\Delta G^0_{rr^*} + (\Delta G^0_{rp} - \Delta G^0_{rr^*} + \lambda_f + \lambda_c)^2/[4(\lambda_f + \lambda_c)]$	$(\Delta G^0_{rr^*} + \lambda_c)^2/(4\lambda_c)$
$R \rightleftharpoons P^* \rightleftharpoons P$	$(\Delta G^0_{rp} + \Delta G^0_{pp^*} + \lambda_f + \lambda_c)^2/[4(\lambda_f + \lambda_c)]$	$\Delta G^0_{rp^*} + (-\Delta G^0_{pp^*} + \lambda_c)^2/(4\lambda_c)$	$(\Delta G^0_{rp} + \Delta G^0_{pp^*} + \lambda_f + \lambda_c)^2/[4(\lambda_f + \lambda_c)]$

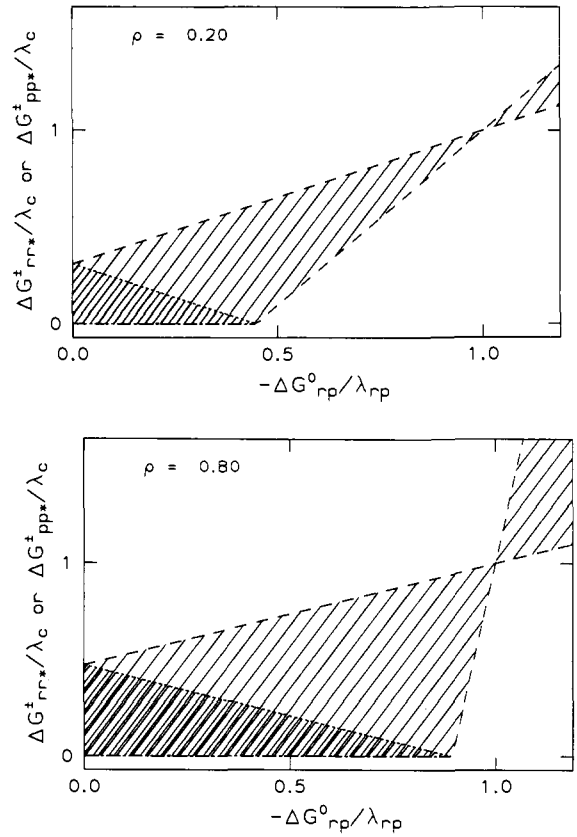

Figure 8. Plot of $\Delta G^{\ddagger}_{rr^*}/\lambda_c$ and $\Delta G^{\ddagger}_{pp^*}/\lambda_c$ vs $\Delta G^0_{rp}/\lambda_{rp}$, where $\Delta G^{\ddagger}_{rr^*}$ and $\Delta G^{\ddagger}_{pp^*}$ are the free energy of the low-λ R* or P* intermediate at which the barriers for the two-step and the direct pathways are equal, ΔG^0_{rp} and λ_{rp} are the free energy change and reorganization parameter, respectively, for the R → P reaction, and λ_c and λ_f are the reorganization parameters for the conformational and fast modes, respectively. The two solutions of $\Delta G^{\ddagger}_{rr^*}$ are shown as short dashes. The solutions for $\Delta G^{\ddagger}_{pp^*}$ are shown as long dashes (at low $\Delta G^0_{rp}/\lambda_{rp}$ the line for $\Delta G^{\ddagger}_{rr^*}/\lambda_f$ overlays the line for $\Delta G^{\ddagger}_{pp^*}/\lambda_f$). The area between the long dashed lines (the total shaded area) is the region in which the low-λ P* mechanism is favored (i.e., values of $\Delta G^0_{pp^*}/\lambda_c$ and $\Delta G^0_{rp}/\lambda_{rp}$ that favor the two-step over the direct mechanism); the area between the short dashed lines (the shaded area of closely spaced lines) shows the region in which the low-λ R* mechanism is favored (i.e., values of $\Delta G^0_{rr^*}/\lambda_c$ and $\Delta G^0_{rp}/\lambda_{rp}$ that favor the two-step over the direct mechanism). For all other regions the direct route has the lowest energy barrier. The top and bottom figures are drawn by using $\rho = \lambda_{r^*p}/\lambda_{rp} = \lambda_{rp^*}/\lambda_{rp} = 0.2$ and 0.8, respectively.

P* mechanism is favored over the direct pathway; in general the P* mechanism is favored only at large values of $\Delta G^0_{pp^*}/\lambda_c$ as seen in Figure 8. Equation 15 can be rearranged to show that the following condition needs to be satisfied for the P* mechanism to be favored:

$$|\Delta G_{rp} + \lambda_{rp}|(1 - \rho^{1/2}) \leq \Delta G^0_{pp^*} - \lambda_{rp}(1 - \rho) \leq |\Delta G^0_{rp} + \lambda_{rp}|(1 + \rho^{1/2})$$

For $\rho \approx 1$ this gives

$$\Delta G^0_{pp^*} \leq 2|\Delta G^0_{rp} + \lambda_{rp}|$$

High-λ Intermediates. While low-λ R* or P* intermediates have lower reorganization parameters for electron transfer than R or P, high-λ intermediates have *higher* reorganization parameters. High-λ R* or P* intermediates can differ from their stable R or P conformers along a coordinate not contributing to the electron-transfer reorganization parameter λ_{rp}. This will introduce

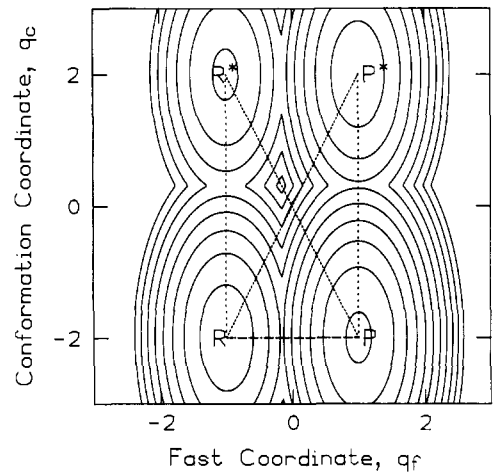

Figure 9. Contour plot of the free energy surface for an electron-transfer reaction in which the reactant R and product P each have an unstable high-λ conformer R* and P*, respectively. The reaction path and the reaction coordinate are the same for the direct R → P reaction. The widely and closely spaced dotted lines show the reaction coordinate for the conformation changes and the electron-transfer reactions, respectively. The surface is drawn assuming that $\Delta G^0_{rr^*} = \Delta G^0_{pp^*} = 0.16\lambda_c$, $\Delta G^0_{rp} = 0.16\lambda_{rp}$, $\rho = 2.0$, and $H_{rp} = 0$. The reactant and product have identical (reduced) force constants, the ratio of the force constant for the conformational coordinate to that of the fast coordinate is 4.

a new contribution to the reorganization parameter for the unstable conformer. High-λ intermediates may also differ from their stable parent along a nuclear coordinate that already contributes to the reorganization parameter of the parent. In the latter case the electron-transfer reaction involving the high-λ R* or P* intermediate must have a larger difference in the equilibrium values of this coordinate than there is between R and P[34] (i.e., $|q^{r^*}_c - q^p_c| > |q^r_c - q^p_c|$ or $|q^r_c - q^{p^*}_c| > |q^r_c - q^p_c|$). Thus high-$\lambda$ and low-λ intermediates can result from changes in the q_c coordinate, but the changes are in the opposite direction and have the effect of increasing λ_c in the high-λ case.

To simplify the remaining discussion, we will assume that the problem can be reduced to two dimensions. The coordinate q_f will be associated with the *net* reorganization in the parent conformer (which may involve several modes), while q_c will be associated with the new contribution to the reorganization parameter introduced by the conformation change. The reaction scheme is shown in eq 6 and 7, and the kinetic analysis shown in Table I applies. The value of the equilibrium nuclear configuration of R* (P*) differs from that of R (P) in only the q_c coordinate; the equilibrium value of this coordinate is the same for R and P. Thus the equilibrium nuclear configurations of R and R* are (q^r_f, q^r_c) and $(q^r_f, q^{r^*}_c)$, respectively, and those of P* and P are $(q^p_f, q^{r^*}_c)$ and (q^p_f, q^r_c), respectively. The reorganization parameter for the direct reaction is $\lambda_{rp} = \lambda_f$ while for the R* and P* mechanisms $\lambda_{r^*p} = \lambda_f + \lambda_c$ and $\lambda_{rp^*} = \lambda_f + \lambda_c$, respectively. A contour plot for the case of high-λ intermediates is shown in Figure 9. The stable reactant and product are shown at the bottom of the plot with the unstable conformers shown at the top. The equilibrium nuclear configurations of R, R*, P*, and P lie at the corners of a rectangle. For the high-λ intermediates the direct electron-transfer reaction is described by motion from R to P along one side of the rectangle while the electron-transfer steps in the two-step mechanisms occur along a diagonal. (This is opposite to the situation for the low-λ intermediates).

The free-energy barriers for the direct and two-step reactions can be obtained from eq 4 by the same procedure used in Table

II. The barriers for the high-λ intermediates are given in Table III.

The expression for the barrier in case 1b of the high-λ R* mechanism shows that the barrier for the electron-transfer step is modified by the larger reorganization parameter, the increase in driving force, and the unfavorable preequilibrium. In the normal region only the increase in driving force favors the two-step reaction, and this effect is more than compensated for by the changes in the other parameters. For the high-λ P* mechanism (case 2) the barrier is modified by the smaller driving force and the increased reorganization parameter. Both changes make the P* mechanism unfavorable with respect to the direct reaction. Two-step reactions utilizing high-λ intermediates are never favorable in the normal free energy region; however, they can become favorable in the inverted region. The barriers for the gated reactions, case 2 of the R* mechanism and case 1b of the P* mechanism, are the same for high-λ and low-λ intermediates.

The barriers for the two-step and direct mechanisms can be compared as was done for low-λ intermediates. The expressions are the same as those for low-λ intermediates, eq 14 and 15, however, the value of the parameter ρ changes:

$$\rho = \frac{\lambda_{r^{\bullet}p}}{\lambda_{rp}} \quad \text{or} \quad \frac{\lambda_{rp^{\bullet}}}{\lambda_{rp}} = \frac{\lambda_f + \lambda_c}{\lambda_f} \geq 1 \tag{18}$$

Only $\Delta G^{-}_{rr^{\bullet}}$ in eq 14 and $\Delta G^{+}_{pp^{\bullet}}$ in eq 15 are physically meaningful.[40] The lowest value of $|\Delta G^0_{rp}|/\lambda_{rp}$ at which either the high-λ R* or P* mechanism ($\Delta G^{\pm}_i/\lambda_c = 0$ intercept) becomes favorable is given by

$$|\Delta G^0_{rp}|/\lambda_{rp} = \rho^{1/2} = (1 + \lambda_c/\lambda_f)^{1/2} \tag{19}$$

This intercept is always >1 (i.e., the R* and P* pathways are favorable only in the inverted region).

High-λ Intermediates: Inverted Region. For either the R* or P* pathway the increase in rate relative to the direct mechanism depends upon $\Delta G^0_{rr^{\bullet}}$ (or $\Delta G^0_{pp^{\bullet}}$) and λ_c. Consider the high-λ P* pathway: both the reduction in the driving force of the electron-transfer step by $\Delta G^0_{pp^{\bullet}}$ (see Table III, case 1a) and the increase in λ_{rp} by λ_c make the reaction less inverted (or even normal) and consequently increase its rate relative to the direct reaction. Equation 19 can be manipulated to show that, at the intercept, the ratio $|\Delta G^0|/\lambda$ for the two-step and direct pathways are related by eq 20. For the R* or P* mechanisms eq 14–16

$$\Delta G^0_{rp}/\lambda_{rp} = \lambda_{r^{\bullet}p}/\Delta G^0_{r^{\bullet}p} = \lambda_{rp^{\bullet}}/\Delta G^0_{rp^{\bullet}} \tag{20}$$

can be rearranged to show that the R* pathway is favorable only when

$$0 < \Delta G^0_{rr^{\bullet}} \leq (\rho^{1/2} - 1)|\Delta G^0_{rp}| - (\rho - \rho^{1/2})\lambda_{rp}$$

$$0 \leq \Delta G^0_{rr^{\bullet}} \leq (\rho^{1/2} + 1)|\Delta G^0_{rp}| - (\rho + \rho^{1/2})\lambda_{rp}$$

For $\rho \approx 1$ (i.e., $\lambda_{rp} \approx \lambda_{rp^{\bullet}}$ and $\lambda_c \ll \lambda_f$) there are no $\Delta G^0_{rr^{\bullet}}$ values for which the R* mechanism is favored. This results because R* is no longer a high-λ intermediate. However, for the P* mechanism there always exist values of $\Delta G^0_{pp^{\bullet}}$ that favor the high-λ mechanism. In general, when $\lambda_{rp^{\bullet}} > \lambda_{rp}$, there are values for $\Delta G^0_{rr^{\bullet}}$ and $\Delta G^0_{pp^{\bullet}}$ that make the R* or P* pathway favorable. This is in contrast to the low-λ case where only the P* pathway can be favorable.

For the high-λ P* mechanism the electron-transfer step will become slow, and the direct electron-transfer reaction will be more favorable when the reduction in the driving force by $\Delta G^0_{pp^{\bullet}}$ or the increase in the reorganization parameter by λ_c is too large. Similar effects are also found for the R* pathway. Figure 10 shows a plot of $\Delta G^{\pm}_{rr^{\bullet}}/\lambda_c$ (or $\Delta G^{\pm}_{pp^{\bullet}}/\lambda_c$) vs $\Delta G^0_{rp}/\lambda_{rp}$ for particular values of ρ. The shaded area again indicates the region where the two-step mechanisms are favorable. As seen in the figure the high-λ R* mechanism is favorable only for R* conformers that are only slightly less stable than R. The high-λ P* mechanism, however, is favored over a larger range of $\Delta G^0_{pp^{\bullet}}$ values. As $\rho \rightarrow 1$, the slopes of eq 14 and 15 become more negative and the lowest value of $\Delta G^0_{rp}/\lambda_{rp}$ for which the two-step mechanism if favored also becomes less negative, thereby increasing the range of $\Delta G^0_{rr^{\bullet}}$ and $\Delta G^0_{pp^{\bullet}}$ values favoring the two-step mechanism.

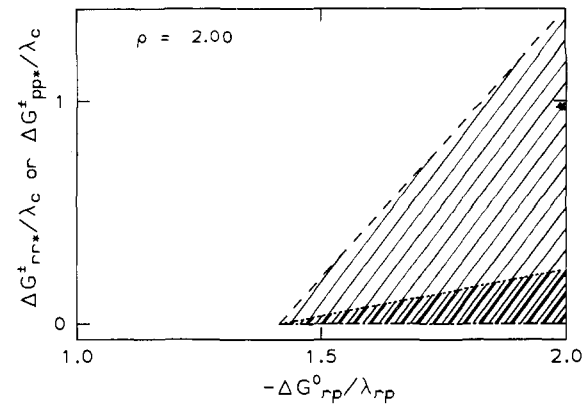

Figure 10. Plot of $\Delta G^{\pm}_{rr^{\bullet}}/\lambda_c$ and $\Delta G^{\pm}_{pp^{\bullet}}/\lambda_c$ vs $\Delta G^0_{rp}/\lambda_{rp}$, where $\Delta G^{\pm}_{rr^{\bullet}}$ and $\Delta G^{\pm}_{pp^{\bullet}}$ are the free energy of the high-λ R* or P* conformer at which the barriers for the two-step and the direct pathways are equal, ΔG^0_{rp} and $\lambda_{rp} = \lambda_f$ are the free energy change and reorganization parameter, respectively, for the direct R → P reaction, and λ_c is the reorganization parameter for the conformational mode. The conformational mode is not active in the direct electron-transfer reaction. The two solutions of $\Delta G^{\pm}_{pp^{\bullet}}$ are shown as long dashes. The solutions of $\Delta G^{\pm}_{rr^{\bullet}}$ are shown as short dashes. The area between the long dashed lines (the total shaded area) is the region in which the P* mechanism is favored (i.e., values of $\Delta G^0_{pp^{\bullet}}/\lambda_c$ and $\Delta G^0_{rp}/\lambda_{rp}$ that favor the two-step over the direct mechanism); the area between the short dashed lines (the shaded area of closely spaced lines) shows the region in the R* mechanism is favored (i.e., values of $\Delta G^0_{rr^{\bullet}}/\lambda_c$ and $\Delta G^0_{rp}/\lambda_{rp}$ that favor the two-step over the direct mechanism). For all other regions the direct route has the lowest energy barrier. The figure is drawn by using $\rho = \lambda_{r^{\bullet}p}/\lambda_{rp} = \lambda_{rp^{\bullet}}/\lambda_{rp} = 2.0$.

Applications

Low-λ Intermediates: Directional Electron Transfer. Because the P* pathway can be favorable for values of λ_f/λ_c and $\Delta G^0_{rp}/\lambda_{rp}$ for which the R* pathway is unfavorable, unusual effects can be observed. Consider the situation for intramolecular electron transfer between two different redox centers A and B (eq 21)

$$A^{-}\text{–}B \xrightarrow{k_{for}} A\text{–}B^{-} \tag{21}$$

where k_{for} is the rate constant for the direct electron transfer from A^- to B. Assume B can be chemically modified to change the driving force for the reaction so that the electron transfer proceeds spontaneously in the reverse direction (eq 22)

$$A\text{–}B^{-}{}_m \xrightarrow{k'_{rev}} A^{-}\text{–}B_m \tag{22}$$

where k'_{rev} is the rate constant for the direct electron transfer from B^-_m to A.

Reactions 21 and 22 have free energy changes ΔG^0_{for} and $\Delta G^{0\prime}_{rev}$, respectively (where the prime will denote the chemically modified system), and the two reactions are assumed to have identical reorganization parameters ($\lambda_{for} = \lambda'_{rev} = \lambda$). The "normal" relationship between the rates for these two direct reactions (assuming identical electronic factors) is given by eq 23.

$$\ln [k_{for}/k'_{rev}] = ((\lambda + \Delta G^0_{for})^2 - (\lambda + \Delta G^{0\prime}_{rev})^2)/(4\lambda) \tag{23}$$

When the driving forces for the two reactions are the same ($\Delta G^0_{for} = \Delta G^{0\prime}_{rev}$), the rate constants will be equal:[42] For such systems the rate of the reaction is independent of the direction of the electron transfer (again assuming identical electronic factors).

(40) The positive root of eq 14 and the negative root of eq 15 yield negative values only for $\Delta G^{\pm}_{pp^{\bullet}}$ or $\Delta G^{\pm}_{rr^{\bullet}}$ when ΔG^0_{rp} is negative.

(41) Wishart, J. F.; Cho, M.; Isied, S. S. In *Abstracts of Thirteenth DOE Solar Photochemistry Research Conference*, Silver Springs, CO, 1989, p 188.

(42) The two back reactions would also have equal rate constants $k_{rev} = k'_{for}$.

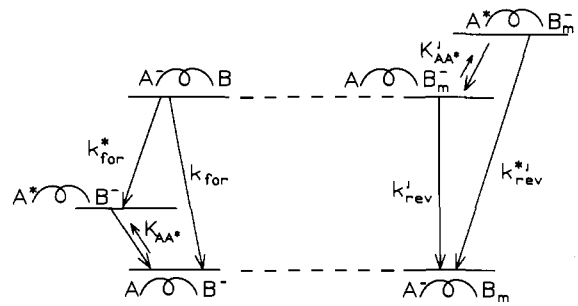

Figure 11. Illustration of the rate constants for the forward intramolecular electron-transfer reaction in the unmodified A–B system and the rate constants for the reverse electron-transfer reaction in the modified A–B_m system.

The introduction of a pathway involving an unstable conformation of A destroys the above symmetry. The energetics of the situation are now shown in Figure 11. In certain situations the pathway through the A* intermediate may be kinetically favorable for the forward reaction but not for the reverse reaction of the chemically modified system. For example, in eq 24 k_{for}(obsd), the observed rate constant for electron transfer from A^- to B, is equal to k^*_{for}, the rate constant for the electron transfer from A^- to B to give A^*-B^- (cf. eq 7 where the second step is assumed to be fast, case 2 of Table I):

$$A^-B \xrightarrow{k^*_{for}} A^*-B^- \xrightleftharpoons{1/K_{AA^*}} A-B^- \qquad (24)$$

However, the observed rate constant for electron transfer within the chemically modified system may still be that of the direct reaction k_{rev}(obsd) = k'_{rev} of eq 22. Since the mechanism for the forward reaction (two-step mechanism) differs from that of the "reverse" reaction (the direct reaction in the chemically modified system), different rate constants may be observed for the forward and "reverse" reactions, i.e., k_{for}(obsd) $\gg$ k'_{rev}(obsd), even though the rate constants for the direct one-step reactions may be equal ($k_{for} = k'_{rev}$). An example of this situation is a reaction having the following parameters: λ_c = 31 kcal mol^{-1}, λ_f = 5 kcal mol^{-1}, $\Delta G^0_{for} = \Delta G^{0\prime}_{rev}$ = −3.5 kcal mol^{-1}, and $\Delta G^0_{AA^*}$ = 6 kcal mol^{-1} ($K_{AA^*} = 4 \times 10^{-5}$). Using these values and assuming that all the electron-transfer steps have the same prefactor (i.e., $\kappa_{el}\nu_n\Gamma_n$ is the same for all the electron-transfer steps) yield barriers for eq 22 and 24 of 2.8 and 7.3 kcal mol^{-1}, respectively. Under these conditions case 2 in Table I applies, and the observed rate constants will differ by more than 3 orders of magnitude:

$$\log\left(\frac{k_{for}(obsd)}{k_{rev}(obsd)}\right) = \log\left(\frac{k^*_{for}}{k'_{rev}}\right) = \frac{7.3 - 2.8}{2.3RT} = 3.3 \qquad (25)$$

The observed rate constants thus depend strongly on the direction of the electron transfer. The barrier for the electron-transfer step shown in eq 26 is less than 1 kcal mol^{-1}, yielding a rate constant

$$A-B^-_m \xrightleftharpoons{K'_{AA^*}} A^*-B^-_m \xrightarrow{k^{*\prime}_{rev}} A^-B_m \qquad (26)$$

for this step that is more than 4 orders of magnitude faster than that of the direct reaction; however, the preequilibrium step in eq 26 is unfavorable by 6 kcal mol^{-1}, resulting in a net rate constant $K'_{AA^*}k^{*\prime}_{rev}$ that is very close to that for the direct reaction (barrier of 7.0 kcal mol^{-1}).

As noted in the introduction, directional electron transfer has been reported for ruthenium-modified cytochrome *c* and may in fact obtain in a variety of conformationally labile metalloprotein systems. In terms of the model discussed here, the reactions of the ruthenium-modified cytochrome *c* may be represented by eq 27 and 28. The electron transfer in the forward direction, eq 27, proceeds by a two-step mechanism in which a rapid (but unobserved) conformation change *succeeds* the electron transfer. The concerted electron transfer is slower than the two-step mechanism in this case. (Alternative mechanisms, in which the concerted mechanism is the faster, can also be written, but it is then impossible to have a common description based only on energetics for the pentaammine and isonicotinamide systems.)

$$(cyt)Fe^{II}-Ru^{II}(NH_3)_5 \xrightarrow{k^*_{for}} *[(cyt)Fe^{II}-Ru^{III}(NH_3)_5] \qquad (27a)$$

$$*[(cyt)Fe^{II}-Ru^{III}(NH_3)_5] \rightleftharpoons (cyt)Fe^{II}-Ru^{III}(NH_3)_5 \qquad (27b)$$

The electron-transfer reaction in the reverse direction, eq 28, may proceed either by the concerted reaction

$$(cyt)Fe^{II}-Ru^{III}(NH_3)_4(isn) \xrightarrow{k'_{rev}} (cyt)Fe^{III}-Ru^{II}(NH_3)_4(isn) \qquad (28a)$$

or by the two-step mechanism in which a rapid conformation change *precedes* the electron transfer:

$$(cyt)Fe^{II}-Ru^{III}(NH_3)_4(isn) \rightleftharpoons *[(cyt)Fe^{II}-Ru^{III}(NH_3)_4(isn)] \qquad (28b)$$

$$*[(cyt)Fe^{II}-Ru^{III}(NH_3)_4(isn)] \xrightarrow{k^{*\prime}_{rev}} (cyt)Fe^{III}-Ru^{II}(NH_3)_4(isn) \qquad (28c)$$

As noted above, it is possible to rationalize electron-transfer rate constants for "forward" and "reverse" reactions that differ by 3 orders of magnitude by postulating a low-λ conformer of one of the species. (No changes in κ_{el} need be invoked.) Recently Isied and Wishart have extended their studies of "forward" and "reverse" electron-transfer rates in derivatized cytochrome *c*.[41] While their new results are still preliminary, the measured rates *cannot* be reproduced by a scheme that involves only λ changes. However, the rate constants can be approximated by a scheme in which a low-λ conformer of the Fe(II) cytochrome *c* has an H_{r^*p} (or H_{rp^*}) that differs from the H_{rp} of the stable conformer. The following parameters yield electron-transfer rate constants close to the observed values: $\kappa_{el_{rp}} \approx 10^{-10}$, $\kappa_{el,r^*_p} = \kappa_{el_{rp^*}} \approx 10^{-6}$, $\lambda_{rp} \approx 1.5$ eV, $\lambda_{r^*p} = \lambda_{rp^*} \approx 0.5$ eV, and $\Delta G^0_{rr^*} = \Delta G^0_{pp^*} \approx 0.5$ eV.

The Incredible Disappearing Inverted Region. Classical electron-transfer theory predicts a decrease in rate with increasing driving force in the inverted free energy region. Although this prediction has received significant confirmation in recent years,[43] there exist many systems for which the observed rate does not decrease with increasing driving force even though $-\Delta G^0_{rp} > \lambda_{rp}$. It has previously been proposed that electronically excited states of the products may play a role in masking the onset of the inverted region.[44] These interpretations have usually focused on reactions in which the reorganization parameters for the excited state are similar to those for the ground state. In the model used here those cases correspond to the formation of a P* intermediate with $\lambda_c = 0$. The P* mechanism now becomes favorable at $\Delta G^0_{rp} = -\lambda_{rp}$ for values of $\Delta G^0_{pp^*} < -2(\Delta G^0_{rp} + \lambda_{rp})$. At larger $\Delta G^0_{pp^*}$ values the P* reaction is too slow due to its small driving force.

As discussed above, the predicted decrease in rate with increasing driving force might be greatly diminished or, perhaps, not even observed at all if high or low-λ intermediates become involved. High-λ intermediates can be effective in either R* or P* pathways. On the other hand, low-λ intermediates allow only a P* pathway to be active. An important difference between the two pathways is the type of reorganization required: for low-λ (P*) intermediates the reorganization must take place in a mode that is active in the R → P electron-transfer reaction while high-λ (R* or P*) intermediates can reorganize in any mode. This increases the likelihood of pathways involving high-λ intermediates.

In the normal free energy region high-λ intermediates are not active, and consequently as the driving force for the electron-transfer reaction is initially increased, the observed rate constant remains that for the direct reaction and increases until a maximum rate is achieved. Through the population of high-λ intermediates the observed rate may then remain at this maximum value despite further increases in driving force (inverted region). This is shown in Figure 12a where the log of the rate constant is plotted vs driving force for the overall reaction: the solid line indicates the rate constant calculated for the direct reaction, the dotted line indicates

(43) Closs, G. L.; Calcaterra, T. L.; Green, N. J.; Penfield, K. W.; Miller, J. R. *J. Phys. Chem.* **1986**, *90*, 3673.
(44) Siders, P.; Marcus, R. A. *J. Phys. Chem.* **1982**, *82*, 622–630.

Table IV. Decay Times and Coefficients Ratios for the Two-Step Mechanism A ⇌ B ⇌ C

	case 1	case 1a	case 1b	case 2
τ_f^{-1}	$k_1 + k_{-1}$	k_1	k_{-1}	$k_2 + k_{-2}$
τ_s^{-1}	$k_{-2} + K_1k_2/(1 + K_1)$	$k_2 + k_{-2}$	$K_1k_2 + k_{-2}$	$k_1 + k_{-1}/(1 + K_2)$
$\mathcal{R}_A$	$K_1 + (1 + K_1)/K_2$	very large	$K_1 + 1/K_2$	very small
$\mathcal{R}_B$	$1 + (1 + K_1)/K_1K_2$	$1 + 1/K_2$	$1 + 1/K_1K_2$	$[K_2/(1 + K_2)][[k_{-1} + k_1(1 + K_2)]/[k_{-1} + (k_1 + k_{-2})(1 + K_2)]]$
$\mathcal{R}_C$	$(k_{-2}/k_{-1})((1 + K_1 + K_1K_2)/(1 + K_1)^2)$	$(k_2 + k_{-2})/k_1$	$(k_{-2}/k_{-1})(1 + K_1K_2)$	$[k_1 + k_{-1}/(1 + K_2)]/(k_2 + k_{-2})$

Table V. Observed Rate Constants for A ⇌ B ⇌ C

mechanism	case 1a $[k_1 \gg k_{-1}, k_2, k_{-2}]$	case 1b $[k_{-1} \gg k_1, k_2, k_{-2}]$	case 2 $[k_2 + k_{-2} \gg k_1 + k_{-1}]$
[A + B] ⇌ C	$k_2 + k_{-2}$	$K_1k_2 + k_{-2}$	$k_1 + k_{-1}/(1 + K_2)$
A ⇌ [B + C]	k_1	$K_1k_2 + k_{-2}$	$k_1 + k_{-1}/(1 + K_2)$

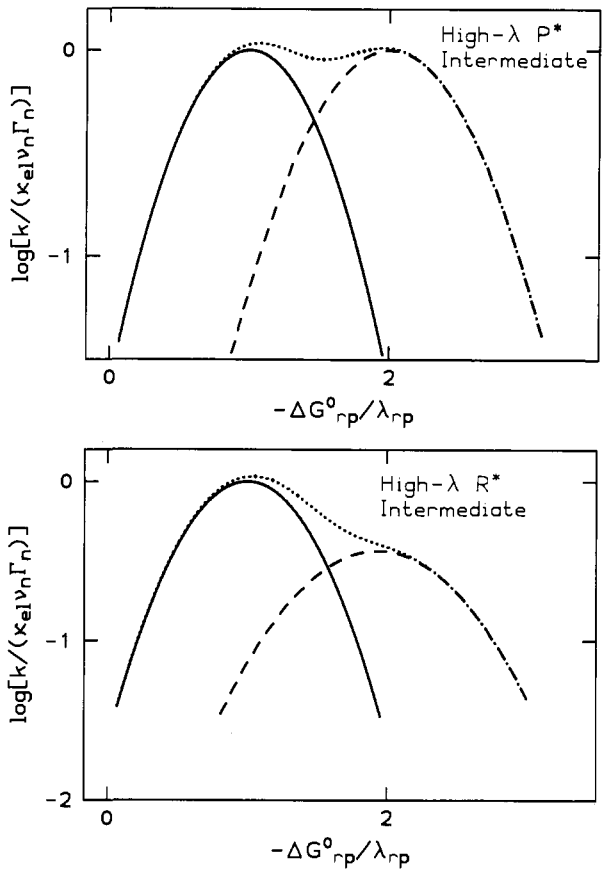

Figure 12. Top: plot of log $[k/(\kappa_{el}\nu_n\Gamma_n)]$ vs $\Delta G^0_{rp}/\lambda_{rp}$ for an electron-transfer reaction with a high-λ P* intermediate. The solid curve describes the direct reaction, the dashed curve describes the high-λ P* mechanism, while the dotted line gives the observed rate constant for the reaction ($k_{obsd} = k_{rp} + k_{rp*}$). The figure is drawn with $\rho = \lambda_{rp*}/\lambda_{rp} = 1.4$, $\lambda_{rp}/RT = 15$, and $\Delta G^0_{pp*}/\lambda_{rp*} = 0.7$. Bottom: plot of log $[k/(\kappa_{el}\nu_n\Gamma_n)]$ vs $\Delta G^0_{rp}/\lambda_{rp}$ for an electron-transfer reaction with a high-λ R* intermediate. The figure is drawn with $\rho = \lambda_{r*p}/\lambda_{rp} = 1.4$, $\lambda_{rp}/RT = 15$, and $\Delta G^0_{rr*}/\lambda_{r*p} = 0.7$.

the observed rate constant for a system that has a high-λ P* intermediate, and the dashed line indicates the rate constant calculated for the P* pathway. Figure 12b shows a similar figure for a system with a high-λ R* intermediate.

The high-λ situation could obtain in photoinduced electron-transfer reactions in modified proteins or in the photosynthetic reaction center.

Conclusions

Criteria have been developed for determining when the direct reaction involving concerted change of the slow (conformational) and fast (vibrational) coordinates is energetically more favorable then pathways involving intermediates. In the normal free energy region, reactions involving high-λ intermediates never compete with the direct reaction. The low-λ R* mechanism is favorable only at low driving force and requires that the R* intermediate be only slightly less stable than R. The low-λ P* mechanism can be favorable over the full free energy region provided that the intermediate's energy ΔG^0_{pp*} falls within certain limits. Because the P* mechanism is favorable over a broader range of free energies and stabilities than the R* mechanism, directional electron transfer can be observed. When one oxidation state of a redox system has an unstable conformer of the appropriate energy, the electron-transfer kinetics may be rapid for electron transfers that can utilize a P* intermediate and slow for electron transfers in the opposite direction where only an R* intermediate is available. This directionality results from the fact that the mechanism for the reaction depends on the direction in which the electron is transferred.

Gating may occur in two-step reactions. However, gating is active only when the conformational deactivation of the intermediate is slower than the electron transfer within the intermediate. This is unlikely for very nonadiabatic electron-transfer reactions. Gating can also give rise to directional electron-transfer.

In the inverted free-energy region, reactions involving low-λ P* and high-λ R* or P* intermediates can compete favorably with direct electron transfer. For the low-λ intermediates a favorable pathway is only provided by those conformers with ΔG^0_{pp*} large enough to make the R → P* reaction less inverted than the direct reaction. On the other hand, for the high-λ intermediates a favorable pathway is only provided by those conformers with ΔG^0_{rr*} or ΔG^0_{pp*} small enough to allow the electron-transfer step of the two-step mechanism to be nearly inverted. Thus while the only low-λ intermediates provide a favorable pathway in the normal free-energy region, pathways with high-λ but relatively stable intermediates can become active in the inverted region. These two-step mechanisms can mask the reduction in rate with increasing driving force expected in the inverted region for the direct reaction.

Acknowledgment. We acknowledge helpful discussions with C. Creutz. This research was carried out at Brookhaven National Laboratory under Contract DE-AC02-76CH00016 with the U.S. Department of Energy and supported by it Division of Chemical Sciences, Office of Basic Energy Sciences.

Appendix A

The two reactions in Scheme I are each of the form

$$A \underset{k_{-1}}{\overset{k_1}{\rightleftharpoons}} B \underset{k_{-2}}{\overset{k_2}{\rightleftharpoons}} C \qquad (A1)$$

where K, K_1, and K_2 are the equilibrium constants for the overall reaction, the first step and the second step, respectively, and $K > 1$. A full kinetic treatment for the above mechanism yields[45]

$$[A] = A_0\left\{k_{-1}k_{-2}\tau_f\tau_s + k_1(1 - k_2\tau_f - k_{-2}\tau_f) \times \left(\frac{\tau_f\tau_s}{\tau_s - \tau_f}\right)e^{-t/\tau_f} - k_1(1 - k_2\tau_s - k_{-2}\tau_s)\left(\frac{\tau_f\tau_s}{\tau_s - \tau_f}\right)e^{-t/\tau_s}\right\} \qquad (A2)$$

(45) Frost, A. A.; Pearson, R. G. *Kinetics and Mechanism* 2nd ed.; Wiley: New York, 1961; pp 175–176.

$$[B] = A_0\left\{k_1k_{-2}\tau_f\tau_s - k_1(1 - k_{-2}\tau_f) \times \left(\frac{\tau_f\tau_s}{\tau_s - \tau_f}\right)e^{-t/\tau_f} + k_1(1 - k_{-2}\tau_s)\left(\frac{\tau_f\tau_s}{\tau_s - \tau_f}\right)e^{-t/\tau_s}\right\} \quad (A3)$$

$$[C] = A_0\left\{k_1k_2\tau_f\tau_s + k_1k_2\tau_f\left(\frac{\tau_f\tau_s}{\tau_s - \tau_f}\right)e^{-t/\tau_f} - k_1k_2\tau_s\left(\frac{\tau_f\tau_s}{\tau_s - \tau_f}\right)e^{-t/\tau_s}\right\} \quad (A4)$$

where A_0 is the total concentration ([A] + [B] + [C]). The decay times τ_f and τ_s are given by eq A5a and A5b[46] and correspond

$$\tau_f^{-1} \approx k_1 + k_{-1} + k_2 + k_{-2} \quad (A5a)$$

$$\tau_s^{-1} \approx \frac{k_1k_2 + k_1k_{-2} + k_{-1}k_{-2}}{k_1 + k_{-1} + k_2 + k_{-2}} \quad (A5b)$$

to the (fast) buildup and (slow) decay of the intermediate, respectively. Two limiting cases are considered in the text. Case 1 applies when $k_1 + k_{-1} \gg k_2 + k_{-2}$, while case 2 applies when the opposite is true. Case 1 is further subdivided depending on whether k_1 (case 1a) or k_{-1} (case 1b) is larger. The two decay times for each case are shown in Table IV. The concentration vs time curve of a particular species will reveal two relaxation times only when the coefficients of the two exponentials (i.e., the coefficients of the second and third terms in eq A2–A4) are of the same magnitude. When one coefficient is much larger than the other, the concentration vs time curve will be dominated by the relaxation time appropriate to that coefficient. The ratio of the coefficients for the fast and slow relaxations for species A, B and C are given by eq A6a–c. The ratio is small when the slow

$$\mathcal{R}_A = \left|\frac{\tau_f(\tau_f^{-1} - k_2 - k_{-2})}{\tau_s(\tau_s^{-1} - k_2 - k_{-2})}\right| \quad (A6a)$$

$$\mathcal{R}_B = \left|\frac{\tau_f(\tau_f^{-1} - k_{-2})}{\tau_s(\tau_s^{-1} - k_{-2})}\right| \quad (A6b)$$

$$\mathcal{R}_C = \frac{\tau_f}{\tau_s} \quad (A6c)$$

relaxation dominates the concentration vs time profile, and it is large when the fast relaxation dominates; when $\mathcal{R} \approx 1$, both relaxations will be observable for that species. $\mathcal{R}_C$ is always small, and the formation of product is dominated by the slower decay time. The ratios of the coefficients for the various cases are given in Table IV.

In the two-step mechanisms of Scheme I we assume that the spectrum of the unstable intermediate (B) does not differ from that of its stable conformer (A or C). This reduces the system to two "effective" species, A and B + C (or A + B and C). The coefficients of the two exponential terms in the equation for the time dependence of the two effective species are equal in magnitude but opposite in sign. Because of this symmetry, only the time dependence of species A (for the case of A and B + C) or of C (for the case of A + B and C) needs to be considered explicitly. (In the discussion below and in the text when reference is made to the time dependence of species A or C it is implied that the two effective species are A and B + C or A + B and C, respectively.) When $k_1 \gg k_{-1}$, case 1a, $\mathcal{R}_A$ will be large with the disappearance of A (and the formation of B + C) dominated by the fast relaxation time, τ_f ($\tau_f^{-1} \approx k_1$). The subsequent slow conversion of B to C is not observable. Alternatively, when $k_{-1} \gg k_1$, case 1b, then $\mathcal{R}_A$ will be small[47] and the disappearance of A depends only upon τ_s ($\tau_s^{-1} = K_1k_2 + k_{-2}$). This is the rapid preequilibrium situation ($K_1 \ll 1$), and a monophasic disappearance of A will be observed. When $k_1 \approx k_{-1}$, $\mathcal{R}_A \approx 1$ and a biphasic decay will be observed. The two phases of the decay will each account for approximately half of the concentration change of A (or of B + C). On the other hand, $\mathcal{R}_C$ is always much less than unity, and the formation of C (and the disappearance of A + B) is primarily determined by the slow relaxation. When the second step in the reaction is fast, case 2, $k_2 + k_{-2} \gg k_1 + k_{-1}$; $\mathcal{R}_A$ is very small and only the slow first step is observable. $\mathcal{R}_C$ is again small, and the formation of C is controlled by the slow formation of B, which then quickly goes on to product. Table V summarizes the rate constants expressions for the limiting cases.

The two-step reaction schemes shown in eq 6 and 7 can be analyzed by using the expressions in Table V. First consider the R* mechanism shown in eq 6. In this mechanism only the formation of product P (or the decay of R + R*) can be detected. For case 1, $k_{rr^\bullet} + k_{r^\bullet r} \gg k_{r^\bullet p} + k_{pr^\bullet}$, but since $k_{r^\bullet r} > k_{rr^\bullet}$ only case 1b is permitted. As shown above only the slow kinetic step will be observed with the rate constant given by (Table V)

$$\tau_s^{-1} \approx K_{rr^\bullet}k_{r^\bullet p} + k_{pr^\bullet} \approx K_{rr^\bullet}k_{r^\bullet p} \quad (A7)$$

where $K_{rr^\bullet}k_{r^\bullet p} \gg k_{pr^\bullet}$.[48] This is the kinetic expression for a fast preequilibrium discussed earlier. When $k_{r^\bullet p} + k_{pr^\bullet} \gg k_{rr^\bullet} + k_{r^\bullet r}$, case 2, product formation is controlled by the slow formation of R*, which rapidly yields the electron-transfer product. The slow conformation change is rate controlling, and the observed rate constant is given by $\tau_s^{-1} \approx k_{rr^\bullet} + k_{r^\bullet r}/K_{r^\bullet p} = k_{rr^\bullet}(1 + 1/K_{rp}) \approx k_{rr^\bullet}$, with $k_{r^\bullet p} \gg k_{pr^\bullet}$ ($K_{r^\bullet p} \gg 1$).

Alternatively, in the P* mechanism (eq 7), only the loss of R (or the formation of P* + P) can be detected. When the forward electron-transfer rate constant is largest, $k_{rp^\bullet} \gg k_{p^\bullet r}, k_{pp^\bullet}, k_{p^\bullet p}$, case 1a, only this fast step will be observed (the conformation change has no absorbance change) with $\tau_f^{-1} \approx k_{rp^\bullet}$. However, when the back-electron-transfer rate constant is largest,[49] $k_{p^\bullet r} \gg k_{rp^\bullet}, k_{pp^\bullet}, k_{p^\bullet p}$, case 1b, only the slow relaxation is observed with $\tau_s^{-1} \approx K_{rp^\bullet}k_{p^\bullet p} + k_{pp^\bullet} = k_{pp^\bullet}(K_{rp} + 1) \approx K_{rp}k_{pp^\bullet} = K_{rp^\bullet}k_{p^\bullet p}$. This is a preequilibrium situation where now the electron-transfer step is in equilibrium and the subsequent slow conformation change is rate limiting. When the free energies of R and P* are similar, then $k_{p^\bullet r} \approx k_{rp^\bullet}$, and two time constants, $\tau_f^{-1} = k_{rp^\bullet} + k_{p^\bullet r}$ and $\tau_s^{-1} = k_{pp^\bullet} + k_{p^\bullet p}k_{rp^\bullet}/(k_{rp^\bullet} + k_{p^\bullet r})$, will be observed. Alternatively, when the conformation change is fast, only the slower electron-transfer step will be observable, $k_{pp^\bullet} + k_{p^\bullet p} \gg k_{rp^\bullet} + k_{p^\bullet r}$ (case 2). The time constant obtained from Table IV is $\tau_s^{-1} \approx k_{rp^\bullet} + K_{pp^\bullet}k_{p^\bullet r}/(1 + K_{pp^\bullet}) \approx k_{rp^\bullet}$, where $k_{p^\bullet p} > k_{pp^\bullet}$ and, due to the energetics of the reaction, $K_{pp^\bullet}k_{p^\bullet r} \ll k_{rp^\bullet}$.[50] Table I summarizes the rate constants for the cases considered above.

(46) The approximation requires that $\tau_f \ll \tau_s$; when this condition is not fulfilled, the more complete expressions must be used: $\tau_f^{-1} = (p + q)/2$ and $\tau_s^{-1} = (p - q)/2$, where $p = k_1 + k_{-1} + k_2 + k_{-2}$ and $q = [p^2 + 4(k_1k_2 + k_1k_{-2} + k_{-1}k_{-2})]^{1/2}$.

(47) Since $K > 1$ and $K_1 \ll 1$, then $K_2 \gg 1$ and $\mathcal{R}_A$ is small.

(48) To show that $K_{pp^\bullet}k_{r^\bullet p} \gg k_{pr^\bullet}$, one uses eq 3–5 for $k_{r^\bullet p}$ and $k_{pr^\bullet}$, along with the expression for the equilibrium constant $K_{pp^\bullet} = \exp(-\Delta G^0_{pp^\bullet}/RT)$. Both $K_{pp^\bullet}k_{r^\bullet p}$ and $k_{pr^\bullet}$ yield expressions of the form $A\exp(-B/RT)$. The prefactor A for each expression is the same. The exponentials B are $\Delta G^0_{rr^\bullet} + [(\Delta G^0_{r^\bullet p} + \lambda_{r^\bullet p})^2/4\lambda_{r^\bullet p}]$ and $(-\Delta G^0_{r^\bullet p} + \lambda_{r^\bullet p})^2/4\lambda_{r^\bullet p}$ for $K_{pp^\bullet}k_{r^\bullet p}$ and $k_{pr^\bullet}$, respectively, where $\lambda_{r^\bullet p}$ is the reorganization parameter for the electron-transfer step and $\Delta G^0_{r^\bullet p}$ is the free energy change for R* → P. After regrouping, the first term becomes $\Delta G^0_{rp} + (-\Delta G^0_{r^\bullet p} + \lambda_{r^\bullet p})^2/4\lambda_{r^\bullet p}$, where $\Delta G^0_{rp} = \Delta G^0_{rr^\bullet} + \Delta G^0_{r^\bullet p}$ is the free energy change for the overall reaction. Since $\Delta G^0_{rp} < 0$, the exponential of the $K_{pp^\bullet}k_{r^\bullet p}$ term is smaller, yielding a larger rate.

(49) In order for $k_{pr^\bullet} > k_{r^\bullet p}$, the free energy change for the reaction $R \rightarrow P^*$ must be positive.

(50) To prove $K_{pp^\bullet}k_{p^\bullet r} \ll k_{rp^\bullet}$, proceed as in ref 43; use eq 3–5 for $k_{rp^\bullet}$ and $k_{p^\bullet r}$ along with the expression for $K_{pp^\bullet}$. Both $K_{pp^\bullet}k_{p^\bullet r}$ and $k_{rp^\bullet}$ yield expressions of the form $A\exp(-B/RT)$. The prefactor A for each expression is the same. For $K_{pp^\bullet}k_{p^\bullet r}$ and $k_{rp^\bullet}$, the exponents B are $[(-\Delta G^0_{rp^\bullet} + \lambda_{rp^\bullet})^2/4\lambda_{rp^\bullet}] - \Delta G^0_{pp^\bullet}$ and $(\Delta G^0_{rp^\bullet} + \lambda_{rp^\bullet})^2/4\lambda_{rp^\bullet}$, respectively, where $\lambda_{rp^\bullet}$ is the reorganization parameter for the electron-transfer step and $\Delta G^0_{rp^\bullet}$ is the free-energy change for R → P*. When the exponential of $K_{pp^\bullet}k_{p^\bullet r}$ is expanded, it reduces to $\Delta G^0_{rp} + (\Delta G^0_{rp^\bullet} + \lambda_{rp^\bullet})^2/4\lambda_{rp^\bullet}$, where $\Delta G^0_{rp} = \Delta G^0_{rp^\bullet} - \Delta G^0_{pp^\bullet}$. Since $\Delta G^0_{rp} < 0$, the exponent of the $K_{pp^\bullet}k_{p^\bullet r}$ term is larger, yielding a smaller rate.